University of Alberta

Seasonal photosynthetic activity in evergreen conifer leaves monitored with spectral reflectance

by

Christopher Yet San Wong

A thesis submitted to the Faculty of Graduate Studies and Research
in partial fulfillment of the requirements for the degree of

Master of Science

Department of Earth and Atmospheric Sciences

Spring 2014
Edmonton, Alberta

Abstract

Annual trends of the Photochemical Reflectance Index (PRI) and pigment content in evergreen conifer leaves were monitored over two years from 2011 to 2013. During the second year, chlorophyll fluorescence and gas exchange were included to examine the spring recovery of photosynthesis. All the metrics indicated large seasonal changes in photosynthetic activity, with a sharp transition in the spring and a more gradual transition in the autumn. The PRI was primarily driven by changes in carotenoid:chlorophyll pigment levels (constitutive processes) that correlated with seasonal photosynthetic activity, with a much smaller variation caused by diurnal changes in xanthophyll cycle activity (facultative processes). Additionally, a previously unrecognized shift in spectral reflectance also affected the PRI under deep cold temperatures. Together, these findings indicate that evergreen conifers photosynthetic system possesses a remarkable degree of resilience in response to large temperature changes across seasons, and that optical remote sensing can be used to observe the seasonal effects on photosynthesis and productivity.

Acknowledgments

This work was supported by funding from Natural Sciences and Engineering Research Council of Canada (NSERC), Alberta Innovates (iCORE) and Canada Foundation for Innovation (CFI).

I would like to express thanks to my supervisor Dr. John A. Gamon for providing me with this opportunity and the invaluable knowledge, guidance and patience he provided. Thank you to Dr. David S. Hik for participating on my committee and providing the idea for examining the spring recovery kinetics. Thank you to Dr. Rolf D. Vinebrooke for participating on my committee and Dr. Tom Chacko in his role as chair of my Master's thesis defense. I would also like to thank Dr. Alexander P. Wolfe for his initial position on my committee. Thanks to Steve Williams for his knowledge and assistance on plant care, Dr. Keith Tierney and his research group for generous usage of laboratory equipment and storage space, Laura Junker and Dr. Ingo Ensminger for their help in the pigment analysis, Saulo Castro and Morgan Randall for initially setting up the plants, and Olga Kovalchuk for her assistance with summer work.

Table of Contents

List of Tables

List of Figures

List of Abbreviations

A – Antheraxanthin

APAR – Absorbed Photosynthetically Active Radiation

Car:Chl – Carotenoid:Chlorophyll Ratio

EPS – Epoxidation State

ETR – Electron Transport Rate

F – Fluorescence

HPLC – High-Performance Liquid Chromatography

J_{max} – RuP_2 Carboxylase Capacity

LUE – Light-Use Efficiency

NPP – Net Primary Productivity

PAR – Photosynthetically Active Radiation

PPFD – Photosynthetic Photon Flux Density

PRI – Photochemical Reflectance Index

V – Violaxanthin

V_{Cmax} – Electron Transport Capacity

Z – Zeaxanthin

Chapter 1. General Introduction

Boreal forests in the northern hemisphere represent approximately 13.7 million square kilometres or ~14% of the terrestrial biosphere and have an important role in the global carbon cycle with net primary productivity (NPP) of about 2.4 Pg C y^{-1} (Field & Raupach, 2004; Bonan, 2008). These forests store about 270 Pg C in total, 79.8 Pg C of which is held in the plants (Field & Raupach, 2004; Pan *et al.*, 2011; Thurner *et al.*, 2014). About one-third of the world's boreal forests are located within Canada, occupying approximately 60% of the total area of the country (Natural Resources Canada, 2009), with an NPP of about 1.02 Pg C y^{-1} (Gonsamo *et al.*, 2013). Their role in carbon sequestration varies as the plants have the ability to act as either a carbon sink by removing carbon or as a source by contributing carbon to the atmosphere (Ciais *et al.*, 1995; Le Quéré *et al.*, 2009).

Historically, the boreal forests of Canada were estimated to be large annual carbon sinks but since the 1970s, carbon uptake rates declined to the point of annual fluctuation between carbon sink or source dynamics (Kurz & Apps, 1999; Goodale *et al.*, 2002; IPCC, 2007; Le Quéré *et al.*, 2009). Since 1990, these forests have acted as a carbon source more frequently and in 2011, they released about 84 million tonnes of carbon (Natural Resources Canada, 2013). Variability between sink and source is dependent on a number of factors including environmental conditions, anthropogenic sources and natural disturbances. The intensity of these factors can affect how the boreal forest contributes to the carbon cycle making it difficult to predict future trends (Kurz *et al.*, 2008b). The ability to monitor an ecosystems role in carbon balance is important as climate change will affect these sink-source dynamics resulting in the uncertainty of the boreal forest's role in the global carbon cycle.

Simple notions suggest a "greening" of northern latitudes with longer growing seasons, but more detailed studies indicate less productive forests associated with drought and climate change (Ciais *et al.*, 2005; Le Quéré *et al.*, 2009). Drier forests due to drought and warming can lead to increased frequency of forest fires, which results in accelerated carbon loss and potential changes in plant composition during recovery (Flannigan *et al.*, 2009; Turetsky *et al.*, 2011). Insect infestations have also caused large episodic carbon releases for certain boreal regions (Ayres & Lombardero, 2000; Kurz *et al.*, 2008a). Warming temperatures are also expected to cause continued northern migration of the boreal treeline (Soja *et al.*, 2007). Changing season length and shifting spring and autumn transitional periods are expected to influence carbon balance but the potential impacts are not well understood (Richardson *et al.*, 2010; Xu *et al.*, 2013). The Boreal Ecosystem-Atmosphere Study (BOREAS) was an international projected started in 1990 to investigate some of these questions regarding the relationship between the boreal forest and the atmosphere. BOREAS improved our understanding of the interactions of the boreal forest and atmosphere, and incorporated new techniques to monitor ecosystem structure and functions (Sellers *et al.*, 1997; Gamon *et al.*, 2004). However, a number of questions still remain for the long-term role of the boreal forest. Feedbacks between the boreal forest, climate and atmosphere are clearly complex and dynamic, causing further uncertainties in the future role of the boreal forests in global biogeochemical cycles and climate.

The boreal forests are characterized by strong seasonality that controls plant photosynthetic and respiratory activity. A short summer season consists of longer photoperiod with high temperatures exceeding 20 ºC, which promotes photosynthesis and growth of the shoots and new leaves. The autumn season consists of decreasing temperatures and shortening photoperiod that signal the plants to undergo cold hardening, an essential stage for surviving winter stress (Levitt, 1980). The long winter season consists of a short photoperiod with low temperatures well below 0 ºC. The spring recovery season of increasing temperatures and photoperiod reactivates growth of the plants (Vogg *et al.*, 1998). The large range of environmental temperature and light conditions between the summer and winter seasons affects the plants' long-term survival strategy and as a result, trees have evolved two different wintertime survival strategies. Deciduous species undergo senescence by losing all their leaves in the autumn to completely shut down for the winter. In contrast, evergreens keep their leaves year round by capitalizing on structural investments. The most prevalent evergreen conifers of the Canadian boreal forests are spruce (*Picea* Mill.) and pine (*Pinus* L.), which can survive up to 800 years in various conditions (Luyssaert *et al.*, 2008). A number of studies on evergreen conifers show that several species including Douglas fir (Ebbert *et al.*, 2005), Ponderosa pine (Verhoeven *et al.*, 1999) and Scots pine (Troeng & Linder, 1982; Leverenz & Öquist, 1987; Filella *et al.*, 2009) demonstrate this seasonal change in photosynthetic activity characterized by winter downregulation and summer activity.

Winter stress consists of a dangerous combination of leaf exposure to low temperatures with periodic high light intensities. Freezing temperatures have the potential for intracellular ice formation, which is a threat to the cell membranes within the leaves (Bigras & Colombo, 2001). To avoid this damage, leaves remove internal water to increase solute concentrations and reduce the risk of freezing (Levitt, 1980). In addition to cold inhibition of the biochemical activity of photosynthesis, the removal of water within the plant inhibits electron transport, ultimately reducing the plants ability to photosynthesize (Öquist & Hüner, 1991; Adams *et al.*, 1995). This photosynthetic downregulation coupled with high light levels in the winter leads to a potentially damaging energy challenge since light energy is still absorbed by the leaves. Absorbed light provides energy for leaves to drive photosynthesis through the excitation of the photosynthetic apparatus, but with the inhibition of photosynthesis in the winter, the leaves face an over-excitation of energy which can result in permanent damage to the photosynthetic apparatus via photoinhibition (Powles, 1984). To prevent this photodamage, the plants undergo cold hardening, signaled by declining temperatures and photoperiod in the autumn, which involves structural and biochemical changes (Levitt, 1980; Larcher & Bauer, 1981; Powles *et al.*, 1983; Powles, 1984; Steponkus, 1984; Guy, 1990; Hüner *et al.*, 1993; Krol *et al.*, 1995; Bigras & Colombo, 2001). These changes allow the leaves to dissipate excess energy to protect the vital structures within the leaves, ensuring their long-term survival.

The sink-source dynamics of plants are controlled by photosynthesis and respiratory activity. Photosynthetic activity is affected by a number of abiotic and biotic factors in the environment that influence the underlying biochemical mechanisms (Berry & Björkman, 1980; Björkman, 1981; Powles & Björkman, 1982). Photosynthesis is initially linearly dependent on photosynthetic photon flux density (PPFD) and at higher levels it becomes non-linear when photosynthesis saturates because of limitations associated with the electron transport rate (Björkman, 1981). In addition, the slope of this relationship can change, which is indicative of varying photosynthetic efficiency (Farquhar *et al.*, 1980). Photosynthetic efficiency changes in the short-term over the course of a day, and in the long-term over different seasons. The variability and complexity of photosynthesis makes it difficult to produce a complete and accurate biochemical model because of the various environmental factors that may affect it (Sellers *et al.*, 1996). The Farquhar *et al.* (1980) model is widely used, but suffers from the fact that it is difficult to parameterize key parameters like RuP_2 carboxylase capacity (J_{max}) and electron transport capacity (V_{Cmax}) due to their dynamics and complexity. For this reason, there is an interest in using optical remote sensing as a “real time indicator” of diurnally and seasonally changing activity.

Global monitoring of vegetation by satellites is being utilized to estimate NPP, which is the annual amount of carbon stored by plants (Cramer *et al.*, 1999).

Satellite methods are usually based on the light use efficiency (LUE) model of Monteith (1977), where productivity (originally called “dry matter yield”) can be predicted from the relationship between absorbed light and plant yield. Various versions of the original model have been created from, some using a standard (fixed) LUE, some varying the LUE with biome (Ruimy *et al.*, 1994), and some using a dynamic LUE driven from meteorological data (Running *et al.*, 2004). Our current understanding of this light-use efficiency is that it’s actually a complex variable instead of a fixed LUE parameter, due to the variability of photosynthetic efficiency with dynamic environmental factors. Current models typically incorporate an adjustable LUE because of its variability within and between species, and across conditions (Sinclair & Horie, 1989; Landsberg & Waring, 1997; Gamon *et al.*, 2001; Garbulsky *et al.*, 2010). Current satellite derived models are incorporating this efficiency parameter (Myneni *et al.*, 2002; Running *et al.*, 2004) but challenges remain in accurately calculating it (Garbulsky *et al.*, 2011; Garbulsky *et al.*, 2013). Satellites use optical reflectance to evaluate the physiological state of plants, and vegetation indices such as the Photochemical Reflectance Index (PRI) have been derived to help calculate the productivity parameters (Gamon *et al.*, 1992).

The PRI was originally devised using proximal optical sampling to monitor short-term diurnal changes of the xanthoplhyll cycle (Fig. 1-1), which is related to LUE (Gamon *et al.*, 1992; Gamon *et al.*, 1993; Peñuelas *et al.*, 1995; Gamon *et al.*, 1997). More recent studies using satellite data have observed that the PRI has weaker correlations with LUE, often varying between vegetation stands (Goerner *et al.*, 2011), which leads to uncertainty in its interpretation. More recent work exploring spring transitions in evergreen conifers calls into questions the synchrony of the PRI with underlying photosynthetic regulation (Porcar-Castell *et al.*, 2012). At the same time, there is a parallel body of literature suggesting a large role for pigment pool sizes in determining seasonal PRI patterns in evergreens, which is related to energy dissipation (Fig. 1-1) (Sims & Gamon, 2002; Stylinski *et al.*, 2002; Filella *et al.*, 2009; Garrity *et al.*, 2011; Porcar-Castell *et al.*, 2012). Clarifying the relative importance of short-term (facultative xanthophyll cycle) and long-term (constitutive pigment pool size) effects in controlling the PRI for evergreen forests was the central focus of this study. To properly utilize satellites in monitoring photosynthetic activity, we need to first understand the physiological features that affect optical signals over the seasonal dynamics. Sorting out the different contributions to the PRI is critical, if we are to use it as a reliable indicator of seasonal photosynthetic activity.

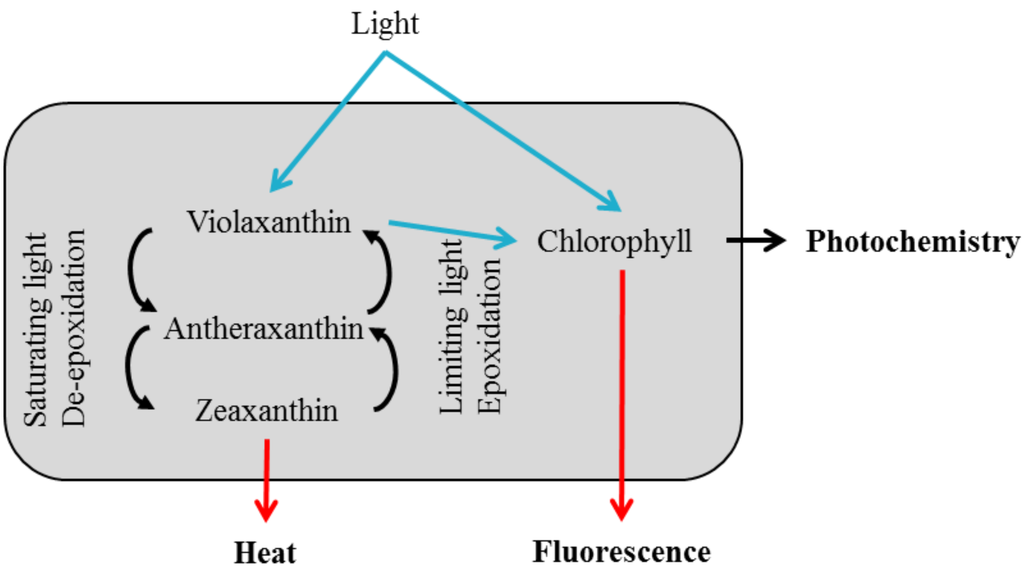

Figure 1-1. Energy flow model of absorbed light energy by the light harvesting complex, based on the models by Butler (1978) and Demmig-Adams (1990). Absorbed light energy by chlorophylls can be used to drive photochemistry or re-emitted by fluorescence. Depending on light conditions, xanthophyll cycle activity can dissipate excess absorbed light as heat. Carotenoids (including xanthophyll cycle pigments) and chlorophylls make up pigment pool sizes associated with overall photosynthetic activity and photoprotection.

This project utilized a number of methods to monitor photosynthetic parameters from evergreen conifers and their seasonal dynamics over two consecutive years. The objectives of this study were to (1) determine the ability of the PRI to track seasonal dynamics in evergreen conifers, (2) evaluate the pigment changes that affect the PRI signal, and (3) determine the relationship of the PRI with other photosynthetic indicators, such as chlorophyll fluorescence and gas exchange. The goal was to evaluate the use of the PRI to estimate photosynthetic activity and address the question of the how to interpret the PRI under dynamic seasonal temperature and light conditions.

Literature Cited

Adams WW, Demmig-Adams B, Verhoeven AS, Barker DH. 1995. Photoinhibion during winter stress: Involvement of sustained xanthophyll cycle-dependent energy dissipation. *Australian Journal of Plant Physiology* **22**(2): 261-276.

Ayres MP, Lombardero MJ. 2000. Assessing the consequences of global change for forest disturbance from herbivores and pathogens. *Science of the Total Environment* **262**(3): 263-286.

Berry J, Björkman O. 1980. Photosynthetic resopnse and adaptation to temperature in higher plants. *Annual Review of Plant Physiology and Plant Molecular Biology* **31**: 491-543.

Bigras FJ, Colombo SJ. 2001. *Conifer cold hardiness*. Dordrecht: Kluwer.

Björkman O. 1981. Responses to different quantum flux densities. In: Lange OL, Nobel PS, Osmond CB, Ziegler H eds. *Physiological Plant Ecology I*: Springer Berlin Heidelberg, 57-107.

Bonan GB. 2008. Forests and climate change: Forcings, feedbacks, and the climate benefits of forests. *Science* **320**(5882): 1444-1449.

Butler WL. 1978. Energy distribution in photochemical apparatus of photosynthesis. *Annual Review of Plant Physiology and Plant Molecular Biology* **29**: 345-378.

Ciais P, Reichstein M, Viovy N, Granier A, Ogée J, Allard V, Aubinet M, Buchmann N, Bernhofer C, Carrara A, Chevallier F, De Noblet N, Friend AD, Friedlingstein P, Grünwald T, Heinesch B, Keronen P, Knohl A, Krinner G, Loustau D, Manca G, Matteucci G, Miglietta F, Ourcival JM, Papale D, Pilegaard K, Rambal S, Seufert G, Soussana JF, Sanz MJ, Schulze ED, Vesala T, Valentini R. 2005. Europe-wide reduction in primary productivity caused by the heat and drought in 2003. *Nature* **437**(7058): 529-533.

Ciais P, Tans PP, Trolier M, White JWC, Francey RJ. 1995. A large northern-hemisphere terrestrial CO_2 sink indicated by the C-13/C-12 ratio of atmospheric CO_2. *Science* **269**(5227): 1098-1102.

Cramer W, Kicklighter DW, Bondeau A, Moore B, Churkina G, Nemry B, Ruimy A, Schloss AL. 1999. Comparing global models of terrestrial net primary productivity (NPP): overview and key results. *Global Change Biology* **5**: 1-15.

Demmig-Adams B. 1990. Carotenoids and photoprotection in plants: A role for the xanthophyll zeaxanthin. *Biochimica Et Biophysica Acta* **1020**(1): 1-24.

Ebbert V, Adams WW, Mattoo AK, Sokolenko A, Demmig-Adams B. 2005. Up-regulation of a photosystem II core protein phosphatase inhibitor and sustained D1 phosphorylation in zeaxanthin-retaining, photoinhibited needles of overwintering Douglas fir. *Plant Cell and Environment* **28**(2): 232-240.

Farquhar GD, von Caemmerer S, Berry JA. 1980. A biochemical model of photosynthetic CO_2 assimilation in leaves of C_3 species. *Planta* **149**(1): 78-90.

Field CB, Raupach R. 2004. *The global carbon cycle: Integrating humans, climate, and the natural world*. Washington, DC: Island Press.

Filella I, Porcar-Castell A, Munné-Bosch S, Bäck J, Garbulsky MF, Peñuelas J. 2009. PRI assessment of long-term changes in carotenoids/chlorophyll ratio and short-term changes in de-epoxidation state of the xanthophyll cycle. *International Journal of Remote Sensing* **30**(17): 4443-4455.

Flannigan M, Stocks B, Turetsky M, Wotton M. 2009. Impacts of climate change on fire activity and fire management in the circumboreal forest. *Global Change Biology* **15**(3): 549-560.

Gamon JA, Field CB, Fredeen AL, Thayer S. 2001. Assessing photosynthetic downregulation in sunflower stands with an optically-based model. *Photosynthesis Research* **67**(1-2): 113-125.

Gamon JA, Filella I, Penuelas J. 1993. The dynamic 531-nanometer delta reflectance signal: a survey of twenty angiosperm species. In: Yamamoto HY, Smith CM eds. *Photosynthetic Responses to the Environment*. Rockville: American Society of Plant Physiologists, 172-177.

Gamon JA, Huemmrich KF, Peddle DR, Chen J, Fuentes D, Hall FG, Kimball JS, Goetz S, Gu J, McDonald KC, Miller JR, Moghaddam M, Rahman AF, Roujean JL, Smith EA, Walthall CL, Zarco-Tejada P, Hu B, Fernandes R, Cihlar J. 2004. Remote sensing in BOREAS: Lessons leamed. *Remote Sensing of Environment* **89**(2): 139-162.

Gamon JA, Peñuelas J, Field CB. 1992. A narrow waveband spectral index that tracks diurnal changes in photosynthetic efficiency. *Remote Sensing of Environment* **41**(1): 35-44.

Gamon JA, Serrano L, Surfus JS. 1997. The photochemical reflectance index: an optical indicator of photosynthetic radiation use efficiency across species, functional types, and nutrient levels. *Oecologia* **112**(4): 492-501.

Garbulsky MF, Peñuelas J, Gamon JA, Inoue Y, Filella I. 2011. The photochemical reflectance index (PRI) and the remote sensing of leaf, canopy and ecosystem radiation use efficiencies A review and meta-analysis. *Remote Sensing of Environment* **115**(2): 281-297.

Garbulsky MF, Peñuelas J, Ogaya R, Filella I. 2013. Leaf and stand-level carbon uptake of a Mediterranean forest estimated using the satellite-derived reflectance indices EVI and PRI. *International Journal of Remote Sensing* **34**(4): 1282-1296.

Garbulsky MF, Peñuelas J, Papale D, Ardö J, Goulden ML, Kiely G, Richardson AD, Rotenberg E, Veenendaal EM, Filella I. 2010. Patterns and controls of the variability of radiation use efficiency and primary productivity across terrestrial ecosystems. *Global Ecology and Biogeography* **19**(2): 253-267.

Garrity SR, Eitel JUH, Vierling LA. 2011. Disentangling the relationships between plant pigments and the photochemical reflectance index reveals a new approach for remote estimation of carotenoid content. *Remote Sensing of Environment* **115**(2): 628-635.

Goerner A, Reichstein M, Tomelleri E, Hanan N, Rambal S, Papale D, Dragoni D, Schmullius C. 2011. Remote sensing of ecosystem light use efficiency with MODIS-based PRI. *Biogeosciences* **8**(1): 189-202.

Gonsamo A, Chen JM, Price DT, Kurz WA, Liu J, Boisvenue C, Hember RA, Wu CY, Chang KH. 2013. Improved assessment of gross and net primary productivity of Canada's landmass. *Journal of Geophysical Research-Biogeosciences* **118**(4): 1546-1560.

Goodale CL, Apps MJ, Birdsey RA, Field CB, Heath LS, Houghton RA, Jenkins JC, Kohlmaier GH, Kurz W, Liu SR, Nabuurs GJ, Nilsson S, Shvidenko AZ. 2002. Forest carbon sinks in the Northern Hemisphere. *Ecological Applications* **12**(3): 891-899.

Guy CL. 1990. Cold acclimation and freezing stress tolerance: Role of protein metabolism. *Annual Review of Plant Physiology and Plant Molecular Biology* **41**: 187-223.

Hüner NPA, Öquist G, Hurry VM, Krol M, Falk S, Griffith M. 1993. Photosynthesis, photoinhibition and low temperature acclimation in cold tolerant plants. *Photosynthesis Research* **37**(1): 19-39.

IPCC. 2007. Solomon S, Qin M, Manning M, Chen Z, Marquis M, Averyt KB, Tignor M, Miller HL, eds. *Climate Change 2007: The Physical Science Basis. Working Group I to the Fourth Assessment Report of the Intergovernmental Panel on Climate Change.* Cambridge, UK: Cambridge University Press.

Krol M, Gray GR, Hurry VM, Öquist G, Malek L, Hüner NPA. 1995. Low temperature stress and photoperiod affect an increased tolerance to photoinhibition in *Pinus banksiana* seedlings. *Canadian Journal of Botany-Revue Canadienne De Botanique* **73**(8): 1119-1127.

Kurz WA, Apps MJ. 1999. A 70-year retrospective analysis of carbon fluxes in the Canadian forest sector. *Ecological Applications* **9**(2): 526-547.

Kurz WA, Dymond CC, Stinson G, Rampley GJ, Neilson ET, Carroll AL, Ebata T, Safranyik L. 2008a. Mountain pine beetle and forest carbon feedback to climate change. *Nature* **452**(7190): 987-990.

Kurz WA, Stinson G, Rampley GJ, Dymond CC, Neilson ET. 2008b. Risk of natural disturbances makes future contribution of Canada's forests to the global carbon cycle highly uncerain. *Proceedings of the National Academy of Sciences of the United States of America* **105**(5): 1551-1555.

Landsberg JJ, Waring RH. 1997. A generalised model of forest productivity using simplified concepts of radiation-use efficiency, carbon balance and partitioning. *Forest Ecology and Management* **95**(3): 209-228.

Larcher W, Bauer H. 1981. Ecological significance of resistance to low temperature. *Encyclopedia of Plant Physiology. New Series. Volume 12A. Physiological plant ecology I. Responses to the physical environment. [Lange, O.L.; Nobel, P.S.; Osmond, C.B.; Ziegler, H. (Editors)]*: 403-437.

Le Quéré C, Raupach MR, Canadell JG, Marland G, Bopp L, Ciais P, Conway TJ, Doney SC, Feely RA, Foster P, Friedlingstein P, Gurney K, Houghton RA, House JI, Huntingford C, Levy PE, Lomas MR, Majkut J, Metzl N, Ometto JP, Peters GP, Prentice IC, Randerson

JT, Running SW, Sarmiento JL, Schuster U, Sitch S, Takahashi T, Viovy N, van der Werf GR, Woodward FI. 2009. Trends in the sources and sinks of carbon dioxide. *Nature Geoscience* **2**(12): 831-836.

Leverenz JW, Öquist G. 1987. Quantum yields of photosynthesis at temperatures between -2 °C and -35 °C in a cold tolerant C_3 plant (*Pinus sylvestris*) during the course of one year. *Plant Cell and Environment* **10**(4): 287-295.

Levitt J. 1980. *Responses of plants to environmental stresses*. New York: Academic Press.

Luyssaert S, Schulze ED, Borner A, Knohl A, Hessenmoller D, Law BE, Ciais P, Grace J. 2008. Old-growth forests as global carbon sinks. *Nature* **455**(7210): 213-215.

Monteith JL. 1977. Climate and efficiency of crop production in Britain. *Philosophical Transactions of the Royal Society of London Series B-Biological Sciences* **281**(980): 277-294.

Myneni RB, Hoffman S, Knyazikhin Y, Privette JL, Glassy J, Tian Y, Wang Y, Song X, Zhang Y, Smith GR, Lotsch A, Friedl M, Morisette JT, Votava P, Nemani RR, Running SW. 2002. Global products of vegetation leaf area and fraction absorbed PAR from year one of MODIS data. *Remote Sensing of Environment* **83**(1-2): 214-231.

Natural Resources Canada. 2009. The Atlas of Canada: Boreal Forest. http://atlas.nrcan.gc.ca/site/english/learningresources/theme_modules/borealforest/index.html

Natural Resources Canada. 2013. The State of Canada's Forests. Annual report 2013.

Öquist G, Hüner NPA. 1991. Effects of cold acclimation on the susceptibility of photosynthesis to photoinhibition in Scots pine and in winter and spring cereals: A fluorescence analysis. *Functional Ecology* **5**(1): 91-100.

Pan YD, Birdsey RA, Fang JY, Houghton R, Kauppi PE, Kurz WA, Phillips OL, Shvidenko A, Lewis SL, Canadell JG, Ciais P, Jackson RB, Pacala SW, McGuire AD, Piao SL, Rautiainen A, Sitch S, Hayes D. 2011. A Large and Persistent Carbon Sink in the World's Forests. *Science* **333**(6045): 988-993.

Peñuelas J, Filella I, Gamon JA. 1995. Assessment of photosynthetic radiation-use efficiency with spectral reflectance. *New Phytologist* **131**(3): 291-296.

Porcar-Castell A, Garcia-Plazaola JI, Nichol CJ, Kolari P, Olascoaga B, Kuusinen N, Fernandez-Marín B, Pulkkinen M, Juurola E, Nikinmaa E. 2012. Physiology of the seasonal relationship between the photochemical reflectance index and photosynthetic light use efficiency. *Oecologia* **170**(2): 313-323.

Powles SB. 1984. Photoinhibition of photosynthesis induced by visible light. *Annual Review of Plant Physiology and Plant Molecular Biology* **35**: 15-44.

Powles SB, Berry JA, Björkman O. 1983. Interaction between light and chilling temperature on the inhibition of photosynthesis in chilling sensitive plants. *Plant Cell and Environment* **6**(2): 117-123.

Powles SB, Björkman O. 1982. Photoinhibition of photosynthesis: Effect on chlorophyll fluorescence at 77K in intact leaves and in chloroplast membranes of *Nerium oleander*. *Planta* **156**(2): 97-107.

Richardson AD, Black TA, Ciais P, Delbart N, Friedl MA, Gobron N, Hollinger DY, Kutsch WL, Longdoz B, Luyssaert S, Migliavacca M, Montagnani L, Munger JW, Moors E, Piao SL, Rebmann C, Reichstein M, Saigusa N, Tomelleri E, Vargas R, Varlagin A. 2010. Influence of spring and autumn phenological transitions on forest ecosystem productivity. *Philosophical Transactions of the Royal Society B-Biological Sciences* **365**(1555): 3227-3246.

Ruimy A, Saugier B, Dedieu G. 1994. Methodology for the estimation of terrestrial net primary production from remotely sensed data. *Journal of Geophysical Research-Atmospheres* **99**(D3): 5263-5283.

Running SW, Nemani RR, Heinsch FA, Zhao MS, Reeves M, Hashimoto H. 2004. A continuous satellite-derived measure of global terrestrial primary production. *Bioscience* **54**(6): 547-560.

Sellers PJ, Bounoua L, Collatz GJ, Randall DA, Dazlich DA, Los SO, Berry JA, Fung I, Tucker CJ, Field CB, Jensen TG. 1996. Comparison of radiative and physiological effects of doubled atmospheric CO_2 on climate. *Science* **271**(5254): 1402-1406.

Sellers PJ, Hall FG, Kelly RD, Black A, Baldocchi D, Berry J, Ryan M, Ranson KJ, Crill PM, Lettenmaier DP, Margolis H, Cihlar J, Newcomer J, Fitzjarrald D, Jarvis PG, Gower ST, Halliwell D, Williams D, Goodison B, Wickland DE, Guertin FE. 1997. BOREAS in 1997: Experiment overview, scientific results, and future directions. *Journal of Geophysical Research-Atmospheres* **102**(D24): 28731-28769.

Sims DA, Gamon JA. 2002. Relationships between leaf pigment content and spectral reflectance across a wide range of species, leaf structures and developmental stages. *Remote Sensing of Environment* **81**(2-3): 337-354.

Sinclair TR, Horie T. 1989. Leaf nitrogen, photosynthesis, and crop radiation use efficiency: A review. *Crop Science* **29**(1): 90-98.

Soja AJ, Tchebakova NM, French NHF, Flannigan MD, Shugart HH, Stocks BJ, Sukhinin AI, Parfenova EI, Chapin FS, Stackhouse PW. 2007. Climate-induced boreal forest change: Predictions versus current observations. *Global and Planetary Change* **56**(3-4): 274-296.

Steponkus PL. 1984. Role of the plasma membrane in freezing injury and cold acclimation. *Annual Review of Plant Physiology and Plant Molecular Biology* **35**: 543-584.

Stylinski CD, Gamon JA, Oechel WC. 2002. Seasonal patterns of reflectance indices, carotenoid pigments and photosynthesis of evergreen chaparral species. *Oecologia* **131**(3): 366-374.

Thurner M, Beer C, Santoro M, Carvalhais N, Wutzler T, Schepaschenko D, Shvidenko A, Kompter E, Ahrens B, Levick SR, Schmullius C. 2014. Carbon stock and density of northern boreal and temperate forests. *Global Ecology and Biogeography* **23**(3): 297-310.

Troeng E, Linder S. 1982. Gas exchange in a 20-year-old stand of Scots pine: I. Net photosynthesis of current and one-year-old shoots within and between seasons. *Physiologia Plantarum* **54**(1): 7-14.

Turetsky MR, Kane ES, Harden JW, Ottmar RD, Manies KL, Hoy E, Kasischke ES. 2011. Recent acceleration of biomass burning and carbon losses in Alaskan forests and peatlands. *Nature Geoscience* **4**(1): 27-31.

Verhoeven AS, Adams WW, Demmig-Adams B. 1999. The xanthophyll cycle and acclimation of *Pinus ponderosa* and *Malva neglecta* to winter stress. *Oecologia* **118**(3): 277-287.

Vogg G, Heim R, Hansen J, Schäfer C, Beck E. 1998. Frost hardening and photosynthetic performance of Scots pine (*Pinus sylvestris* L.) needles. I. Seasonal changes in the photosynthetic apparatus and its function. *Planta* **204**(2): 193-200.

Xu L, Myneni RB, Chapin FS, Callaghan TV, Pinzon JE, Tucker CJ, Zhu Z, Bi J, Ciais P, Tømmervik H, Euskirchen ES, Forbes BC, Piao SL, Anderson BT, Ganguly S, Nemani RR, Goetz SJ, Beck PSA, Bunn AG, Cao C, Stroeve JC. 2013. Temperature and vegetation seasonality diminishment over northern lands. *Nature Climate Change* **3**(6): 581-586.

Chapter 2. Three Primary Causes of Variation in the Photochemical Reflectance Index (PRI) Associated with Changing Temperature and Irradiance

Introduction

Established forests cover about 30% of the world's land surface storing about 861 Pg C, 32% of which is stored within the boreal forests (Bonan, 2008; Pan *et al.*, 2011). Evergreen conifers are dominant trees of boreal regions in the northern hemisphere. These forests are characterized by strong seasonality in their photosynthetic and respiratory activity, and are subject to periodic stresses that lead to interannual variability in their role in the global carbon cycle (Goodale *et al.*, 2002). Seasonal variations of light and temperature levels control their photosynthetic activity, which cycles between an active growth period in the summer and dormancy in the winter (Vogg *et al.*, 1998). Evergreens survive through a range of environmental stresses varying between the extremities of each season and this requires physiological acclimation to retain their leaves for the long-term.

Leaves adjust their physiological mechanisms to maintain a balance between light harvesting, photosynthesis and photoprotection (Hüner *et al.*, 1993). The exposure of leaves to light energy is the primary driver of this energy balance and whenever they are exposed to high amounts of light where light absorption exceeds the capacity of photosynthesis, they are susceptible to permanent photodamage to the photosynthetic apparatus (Osmond, 1981; Björkman & Demmig-Adams, 1994; Horton *et al.*, 1996; Hüner *et al.*, 1998). To maintain energy balance via photoprotection, plants can re-emit excess energy through chlorophyll fluorescence or dissipate it as heat (Butler, 1978). Seasonal variation of photosynthetic activity due to changing temperature and photoperiod results in a substantial shift of the energy balance (Öquist & Hüner, 2003). The long winter season of the boreal region is a period of cold temperature stress that leads to photosynthetic downregulation (Levitt, 1980; Bigras & Colombo, 2001). To avoid winter damage, the leaves undergo cold hardening in the autumn, which is signalled by declining temperatures and photoperiod (Öquist & Hüner, 2003). This phase involves increases in the carotenoid pigment pool size, which is correlated with photoprotection (Demmig-Adams & Adams, 1996). Chlorophyll reduction and reorganization has also been reported, which reduces excess energy (Ottander *et al.*, 1995; Adams *et al.*, 2002).

Seasonal and diurnal energy dissipation involves the acclimation of pigments, which also affects the optical properties of the leaves. The Photochemical Reflectance Index (PRI) has been used as an optical proxy of photosynthetic pigment activity and associated light use efficiency due to its detection of the xanthophyll cycle pigment interconversion (Gamon *et al.*, 1992; Peñuelas *et al.*, 1995). The PRI has been studied extensively at a diurnal scale, exhibiting strong correlation with photosynthetic light-use efficiency with changing irradiance during a single day (Gamon *et al.*, 1992; Peñuelas *et al.*, 1995; Gamon *et al.*, 1997). The seasonal component of the PRI is largely correlated with variations in the pigment pool sizes (Sims & Gamon, 2002; Stylinski *et al.*, 2002; Filella *et al.*, 2009; Porcar-Castell *et al.*, 2012). From these studies we conclude that pigment concentrations are often key drivers of the PRI, whether it is from the conversion of the xanthophyll cycle or from changing pigment pool sizes. These pigment responses can be classified based on two different time scales as the short-term xanthophyll cycle (facultative) and long-term pigment pool size (constitutive) adjustments (Gamon & Berry, 2012). Presumably, pigment levels have a role in light energy balance, which ultimately affects the PRI. However, partitioning the diurnal (facultative) and seasonal (constitutive) effects on the PRI has not been as well studied as the diurnal effects, which have received most attention. Both facultative and constitutive responses may vary seasonally to different extents confounding the physiological interpretation of the PRI.

The diurnal response of energy dissipation via the xanthophyll cycle is a dynamic process driven largely by diurnally changing light conditions. Plants experience highest light levels near solar noon, resulting in increased light absorption that exceeds the capacity to utilize it, leading to energy imbalance. To dissipate excess energy, the xanthophyll cycle responds rapidly (within seconds to minutes) to provide photoprotection throughout the day through the de-epoxidation of violaxanthin into zeaxanthin via antheraxanthin (Demmig-Adams & Adams, 1992). At lower light levels in the evening, epoxidation takes place to reverse the cycle. This process of readily reversible dissipation maintains a balance between useful photochemistry and protective energy dissipation throughout a single day under varying light conditions. The interconversion of the xanthophyll cycle affects spectral reflectance near 531 nm, a wavelength used in the PRI, and is correlated with light-use efficiency over the diurnal time scale

(Gamon *et al.*, 1992; Gamon *et al.*, 1993; Peñuelas *et al.*, 1995; Filella *et al.*, 1996; Gamon *et al.*, 1997). These results using proximal optical sampling have led to much speculation that the PRI might serve as an indicator of photosynthetic light-use efficiency from space-borne satellites (Grace *et al.*, 2007; Coops *et al.*, 2010), although a number of challenges have been identified (Barton & North, 2001). Below we examine the prospects of the PRI as a remote index of photosynthetic activity.

Remote sensing provides a way to measure processes related to photosynthetic pigments over a range of spatial and temporal scales. Many studies have indicated significant correlations between the PRI and light-use efficiency at the landscape level (Nichol *et al.*, 2000; Rahman *et al.*, 2001; Hilker *et al.*, 2008; Goerner *et al.*, 2009), but these correlations may vary between vegetation stands (Goerner *et al.*, 2011). Variations over seasonal time spans or across canopies are often linked to changing environmental conditions such as nutrient, water and temperature stress (Gamon *et al.*, 1997; Stylinski *et al.*, 2002; Filella *et al.*, 2004; Sims *et al.*, 2006; Garrity *et al.*, 2011; Porcar-Castell *et al.*, 2012). In evergreens, the PRI and photosystem II light-use efficiency relationship also decouples during the transitional spring period (Porcar-Castell *et al.*, 2012), suggesting other factors besides xanthophyll pigment conversion may be driving the PRI signal during these transitions. Together, the various factors that can influence the PRI can cause variability in the relationship between light-use efficiency and the PRI across different sampling contexts (Garbulsky *et al.*, 2011; Goerner *et al.*, 2011). These confounding effects, while previously well described from a theoretical perspective (Barton & North, 2001) have not always been fully clarified for particular study contexts. Many remote sensing PRI studies simply do not perform the ground validation or experimental measurements needed to link the PRI to the physiological mechanism driving PRI variability. Consequently, the physiological interpretation of the PRI in a remote sensing context remains uncertain.

The aim of this study was to investigate the mechanisms behind annual PRI variation by assessing the PRI and changes in pigment concentrations in conifers at a range of temporal scales over the annual cycle. Based on previous observations linking the PRI to seasonally changing pigment pools (Sims & Gamon, 2002; Stylinski *et al.*, 2002; Filella *et al.*, 2009; Garrity *et al.*, 2011; Porcar-Castell *et al.*, 2012), we hypothesized the PRI would primarily reflect the seasonal dynamics of carotenoid and chlorophyll pigment pool sizes (i.e., constitutive process) rather than the epoxidation state (EPS) of the xanthophyll cycle (i.e., facultative process). We followed the seasonal PRI patterns in the needles of Lodgepole pine (*Pinus contorta* D.) and Ponderosa pine (*Pinus ponderosa* Laws.) undergoing strong seasonal and daily acclimation of photoprotection in response to boreal climate ranging from daily mean temperatures of -30 °C to +30 °C. The absolute diurnal change (facultative component) was also monitored seasonally to partition the two temporal responses of evergreens. In addition, we examined the effect of deep winter cold on the PRI response. We expected that the PRI would track seasonal dynamics in boreal climate and had a particular goal of addressing the constitutive and facultative components. In a subsequent chapter, we investigate the links between the PRI and photosynthetic activity to see if PRI could be a reliable index of seasonal photosynthetic transitions in evergreen conifers.

Materials and Methods

Two conifer species, Lodgepole pine (*Pinus contorta* D.) and Ponderosa pine (*Pinus ponderosa* Laws.) were grown outside at the University of Alberta, Canada. During the summer of 2010, one year old seedlings were planted in a 1:2 soil mixture of sandy top soil and sunshine mix (Sunshine Mix 4, Sun Gro Horticulture, Agawam, MA, USA) with added slow release fertilizer (Nutricote 14-14-14, Sun Gro Horticulture, Agawam, MA, USA). They were potted in 2.31 L pots (CP412CH, Stuewe & Sons, Tangent, OR, USA) and arranged by species into synthetic stands (1.5 m x 1.5 m plots) for their long-term acclimation. To maintain adequate rooting volume and avoid water or nutrient stress, these plants were repotted using fresh soil in the summer of 2011 into medium 2.83 L (TP414, Stuewe & Sons, Tangent, OR, USA) and in the summer of 2012 into large 6.23 L pots (TP616, Stuewe & Sons, Tangent, OR, USA). The plants were watered daily throughout the non-freezing periods to avoid water stress. During winter, extra pots of soil and a plywood frame were added to the outside edges of the plots, and a 3 cm layer of peat moss was added to the soil surface of all pots to provide additional insulation to the roots during winter cold. Data collection took place over a two-year period from August 2011 to July 2013. Young, fully developed needles from the current year’s cohort at the top of the canopy were used throughout the experiment to keep growth light conditions consistently high and to avoid interference of shading effects at different elevations within a canopy.

A weather station provided photosynthetic photon flux density (PPFD) (S-LIB-M003, Onset, Bourne, MA, USA) and air temperature (S-THB-M002, Onset, Bourne, MA, USA) that were collected every minute on a datalogger (U30-NRC, Onset, Bourne, MA, USA). The weather data were aggregated into 15 minute averages that were later expressed as daily averages. The sensors were set up at the same height as the canopy and located within 3-5 m to provide representative conditions of incoming PPFD and ambient temperatures experienced by the leaves.

A spectrometer (UniSpec-SC, PP Systems, Amesbury, MA, USA) operated using a palmtop PC (1000CX, Hewlett-Packard Company, Palo Alto, CA, USA) equipped with a bifurcated fibre optic (UNI410, PP Systems, Amesbury, MA, USA) was used to measure spectral reflectance. A needle leaf clip (UNI501, PP Systems, Amesbury, MA, USA) was utilized to hold the fibre tip at a fixed angle and position relative to the leaf surface to ensure repeatable technique and enable reflectance sampling of individual needles (0.6 mm diameter spot size). Each measurement was preceded by a dark measurement and white reference scan (Spectralon, Labsphere, North Sutton, NH, USA), and reflectance was calculated from each leaf scan divided by a white reference scan after correction for dark current. The integration time was set to 50 ms and 10 successive scans were automatically averaged for each measurement. The PRI was calculated as:

$$PRI = \frac{R_{531} - R_{570}}{R_{531} + R_{570}} \tag{1}$$

R indicates reflectance, and the subscript indicates the waveband in nm. Reflectance at 531 nm can detect subtle changes in the carotenoid pigments of the xanthophyll cycle that correlates with light-use efficiency, and reflectance at 570 nm is insensitive to these changes and used as a reference (Gamon *et al.*, 1992; Gamon *et al.*, 1993; Peñuelas *et al.*, 1995; Gamon *et al.*, 1997). Six randomly selected plants were monitored for the entire study. Five random leaves per plant were measured providing a total sample size of 30 for each sampling period suitable for representation of the canopy, under similar light conditions.

Leaves for pigment assays were collected within 30 minutes of the spectral measurements under similar light and temperature conditions. The leaves were cut into three 1 cm long segments, measured with a fine caliper for leaf area and immediately stored in liquid nitrogen. Leaf samples were later transferred to a -80 °C freezer for long-term storage. For pigment analyses, batches of 6 leaf samples from a given date and time were pooled together and analyzed using high-performance liquid chromatography (HPLC) (1260 Infinity, Agilent Technologies, Santa Clara, CA, USA). HPLC sampling following the Thayer and Björkman (1990) method was used to find the pigment concentrations of various carotenoid and chlorophyll pigments. The HPLC system was calibrated using pigment standards from DHI (DHI LAB Products, Hørsholm, Denmark). The carotenoid:chlorophyll ratio was calculated as the sum of all carotenoids, including neoxanthin, violaxanthin, antheraxanthin, lutein, zeaxanthin and β-carotene, expressed on a total chlorophyll (a and b) basis (mmol mol^{-1}). The epoxidation state (EPS) of the xanthophyll cycle was calculated as:

$$EPS = \frac{V + 0.5A}{V + A + Z} \tag{2}$$

The EPS is an expression of the non-photoprotective pigment composition of the xanthophyll cycle. The letters indicate absolute concentration (µmol m^{-2}) of each xanthophyll pigment violaxanthin (V), antheraxanthin (A) and zeaxanthin (Z).

To examine the variation of the diurnal response across seasons, we measured the absolute diurnal change of the PRI and the EPS of the xanthophyll cycle. Pre-dawn measurements were completed an hour before sunrise for dark-adapted leaves, and afternoon measurements were collected around 13:00 for the light-adapted leaves at high PPFD levels. Optical measurements had a sample size of 30 (five leaves per plant from six plants) and the pigment analysis pooled together 6 leaf segments (one segment per leaf from six plants). The delta response was calculated as dark- minus light-adapted values to measure absolute diurnal change. These measurements were performed on a monthly basis from October 2012 to March 2013 and on a weekly basis from March 2013 to July 2013 for more emphasis on the spring recovery.

The seasonal acclimation of pigments and the PRI was monitored for both evergreen species on a weekly basis from August 2011 to July 2013. Data collection of both spectral reflectance and leaf samples were performed from about 12:00 to 14:00 (within 1-2 hours of solar noon) to avoid self-shading and ensure light conditions were consistently high during midday sampling. Whenever possible, midday samples were taken under sunny conditions to ensure consistent high light during midday sample collection. To examine the magnitude of different PRI responses, changes in PRI (ΔPRI) were calculated three ways: the seasonal response was calculated as the maximal summer minus minimal winter values; the diurnal PRI response was expressed as pre-dawn minus noon values from the same day; and the deep cold response as normal winter (0 to -5 °C) minus deep cold values (<-5 °C) from averages of 30 values sampled less than a week apart.

Results

Over the two-year period, daily mean temperature and PPFD levels exhibited large seasonal variation (Fig. 2-1a). The summer season consisted of stable warm daily average temperatures greater than 20 °C and high daily PPFD averages of 700 µmol m^{-2} s^{-1} due to longer photoperiod and higher solar elevation from June to August. The winter season consisted of lower daily average temperatures well below 0 °C and low daily PPFD averages of 10 µmol m^{-2} s^{-1} due to shorter photoperiod and lower solar elevation from December to March. The autumn transition period from the summer to winter climate occurred gradually from October to November, whereas the spring transition from the winter to summer climate occurred more rapidly during late April and early May.

In both evergreen species, the PRI followed similar seasonal patterns as temperature (Fig. 2-1b) and carotenoid:chlorophyll ratios (Fig. 2-1c). The PRI was highest in the summer and lowest in the winter. The PRI transition in the autumn was more gradual (over two months) than the rapid spring recovery period, which occurred over one month. The carotenoid:chlorophyll ratios displayed an inverse pattern with the highest values in the winter (Fig. 2-1c). These seasonal patterns of repeated across both study years and across leaf age cohorts (Fig. 2-1b,c).

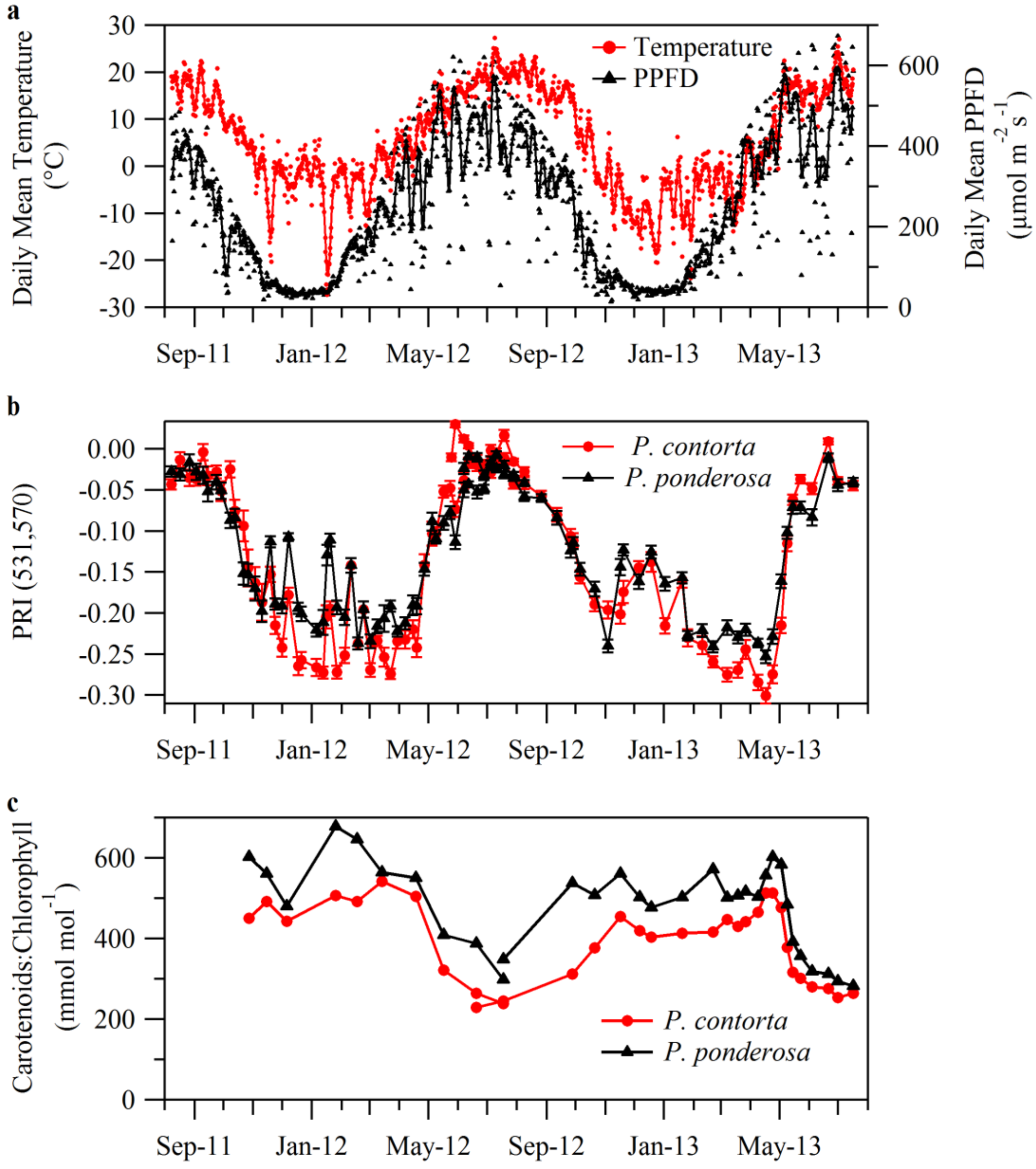

Figure 2-1. Seasonal dynamics of temperature and photosynthetic photon flux density (PPFD) over two years in Edmonton, AB (a). Temperature and PPFD are expressed as daily means as well as the 5-day running mean. Red circles denote daily mean temperature and black triangles denote daily mean of incoming PPFD. The PRI (b) and the total carotenoid concentrations relative to chlorophyll (c) of *P. contorta* (red circle) and *P. ponderosa* (black triangle) over the course of two years. All measurements were obtained near midday. Data overlaps during the summer of 2012 are due to the transition of measurements a new cohort of leaves emerging in 2012. Error bars denote the standard error of the mean (n = 30). Since leaves were pooled for pigment analysis, no error bars are available in panel c (n = 6).

Seasonal changes were visibly observable as the needles went from a bright green colour in the warm summer season to a dull yellow-green colour in the cold winter season. Over the same period, needle reflectance spectra also exhibited seasonal changes across most of the visible and near-infrared regions (Fig. 2-2). The winter-adapted leaves had higher reflectance across most wavelengths. In the visible range, the yellow-red region (550-690 nm) exhibited a large increase and the blue-green region (520-540 nm) displayed a subtle decrease. At the red-edge near 700 nm, winter-adapted leaves had higher reflectance that continued into the near-infrared regions. These seasonal reflectance changes influenced the wavebands used for the PRI calculation (shown as vertical dotted lines in Fig. 2-2); a decrease was observed at 531 nm and an increase occurred at 570 nm in the winter-adapted leaves relative to summer leaves.

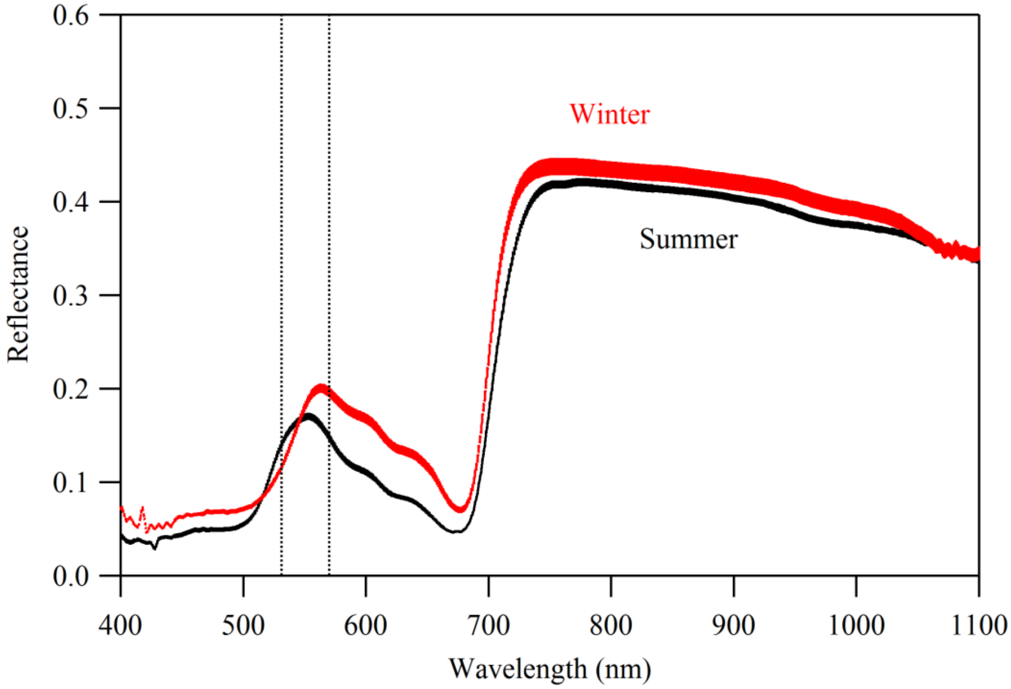

Figure 2-2. Leaf spectra of *P. contorta* showing the seasonal changes between summer- (black) and winter-adapted leaves (red) (n = 30). Vertical dashed lines denote location of PRI wavebands 531 and 570 nm. Line thickness denotes standard error of the mean. Summer spectra from 2011-08-17 and winter spectra from 2011-12-17.

The diurnal response of leaf spectra between dark- and light-adapted leaves was small compared to the seasonal response. The dark- and light-adapted spectra were very similar across all wavelengths (Fig. 2-3). The wavebands of the PRI at 531 nm (the xanthophyll cycle wavelength) exhibited a small decrease in towards midday and no appreciable change at 570 nm (the reference). Slight differences were observed in the near-infrared regions where light-adapted leaves had higher reflectance.

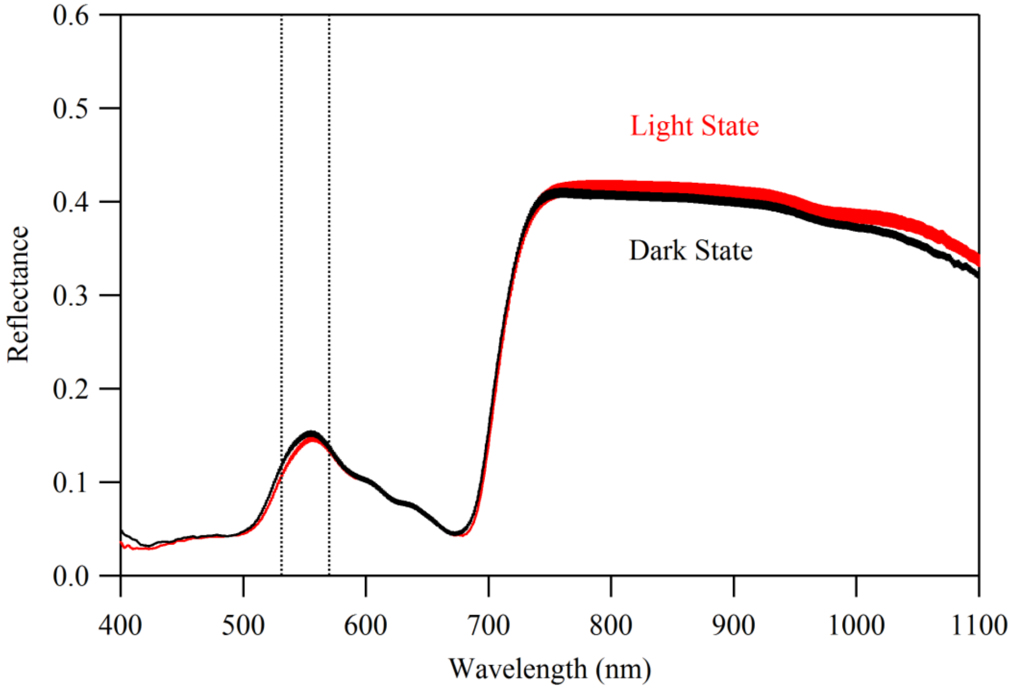

Figure 2-3. Leaf spectra of *P. contorta* showing the diurnal changes between dark- and light-adapted leaves. Vertical dashed lines denote location of PRI wavebands 531 and 570 nm. Line thickness denotes standard error of the mean.

Deep cold also had a strong effect on reflectance and the PRI. During periods of deep cold (<-5 °C), leaf albedo immediately decreased by about half (Fig. 2-4), and these decreases readily reversed when temperatures increased (not shown). During transitions to deep cold, the PRI responded with an abrupt increase of about 0.13 (Fig. 2-1b). Both wavebands of the PRI decreased substantially during the deep cold transitions (see vertical dotted lines, Fig. 2-4). The PRI reversed back to normal winter values each time temperatures reverted above the -5 °C threshold, along with a concurrent increase of leaf albedo (not shown). During the early months of the second winter in the study, December 2012 and January 2013, temperature conditions remained in a sustained deep cold for several weeks, leading to an enhanced PRI during the early part of the second winter season (Fig. 2-1b). Independent experiments (see Appendix A) indicated that the deep cold response and subsequent recovery both occurred very rapidly (within minutes) each time the -5 °C threshold was crossed. Independent tests were performed to confirm that no instrument freezing malfunction occurred and this was indeed a biological response (see Appendix A).

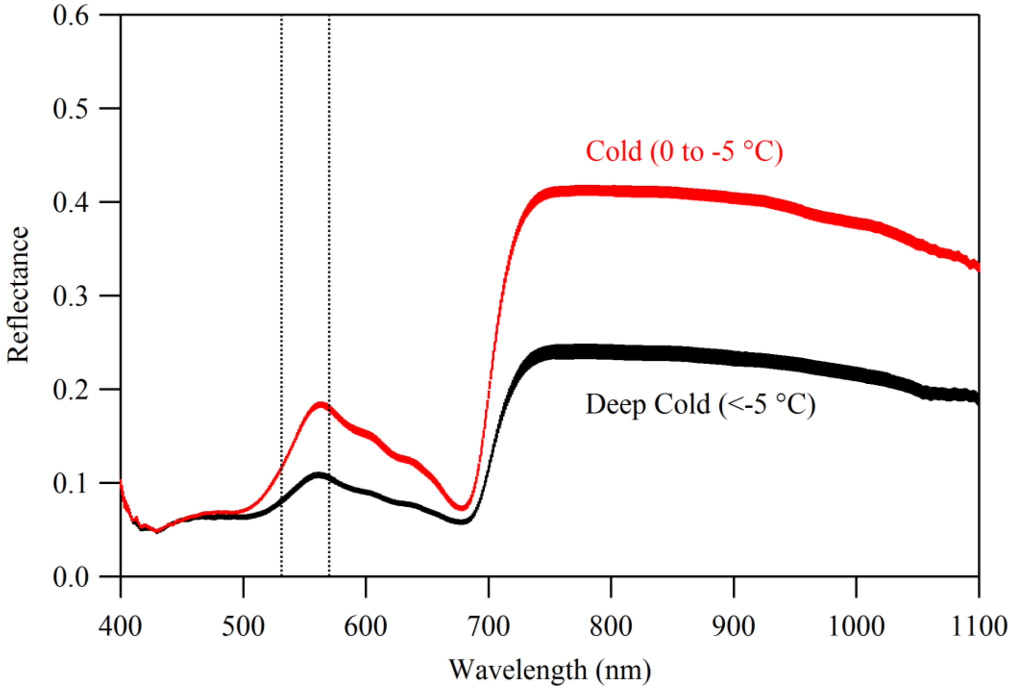

Figure 2-4. Leaf spectra of *P. contorta* in the winter showing a decrease in reflectance during periods of deep cold temperatures (<-5 °C) compared to cool winter temperatures (0 to -5 °C). Vertical dashed lines denote location of PRI wavebands 531 and 570 nm. Line thickness denotes standard error of the mean.

Spectral changes at the three PRI responses (seasonal, diurnal and deep cold) exhibited very different responses to the wavebands of the PRI at 531 and 570 nm. The seasonal component of summer- and winter-adapted leaves had changes in the opposite direction for the two wavebands (Fig. 2-5g). The deep cold component exhibited large changes in the same direction for both wavebands with 570 nm exhibiting a larger change (Fig. 2-5h). The diurnal component displayed a change at 531 nm and negligible difference at 570 nm (Fig. 2-5i).

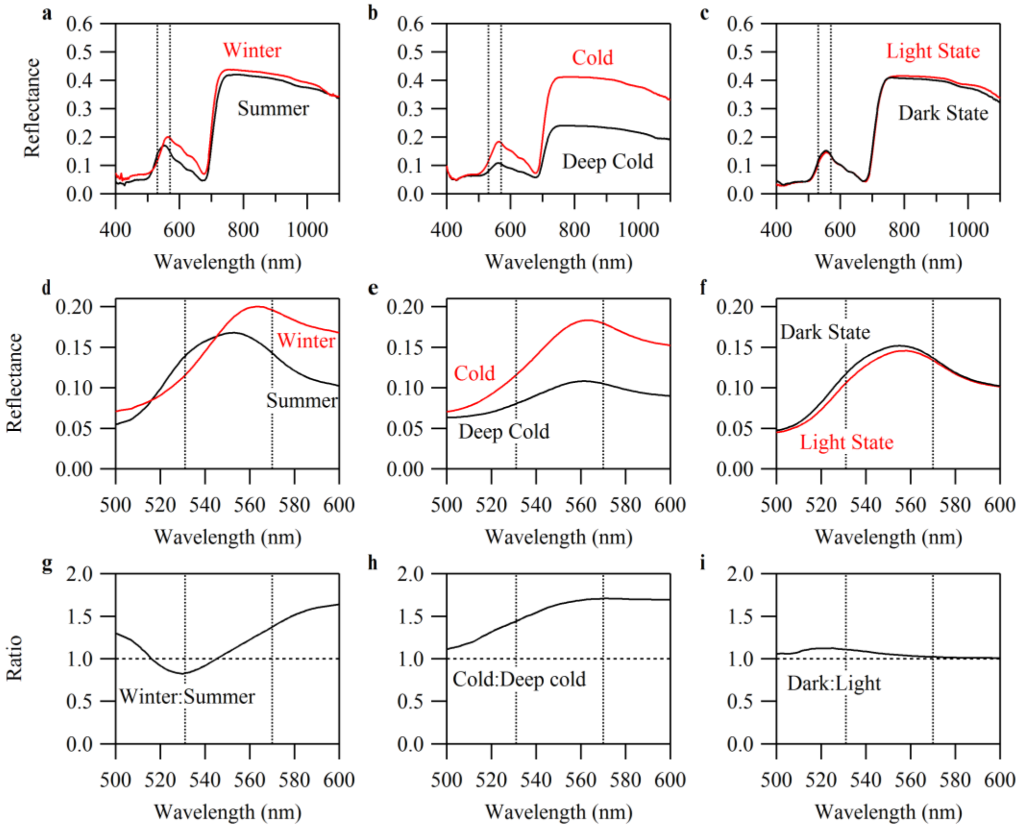

Figure 2-5. Leaf spectra of P. contorta at three temporal scales of seasonal (left; a,d,g), deep cold (<-5 °C) (middle vertical; b,e,h) and diurnal (right; c,f,i). Top panels (a,b,c) are leaf reflectance spectra of the visible and near-infrared regions. Middle horizontal panels (d,e,f) are leaf reflectance spectra expanded from 500 to 600 nm. Bottom panels (g,h,i) are the ratio of the temporal change in reflectance. Vertical dashed lines denote location of the PRI wavebands 531 and 570 nm.

To partition the diurnal and seasonal response of the PRI, we compared the absolute values of the PRI variation in three different contexts: seasonal change, deep cold transitions, and diurnal change (Fig. 2-6). For both species the seasonal delta PRI between the summer and winter states made up the largest variability ranging around 0.25 to 0.34. The deep cold delta response at extreme temperature shifts contributed the second highest variability ranging from 0.10 to 0.15. The diurnal variability of the PRI was the smallest ranging from 0.04 to 0.08. *P. contorta* had slightly higher variability of the PRI for all temporal components.

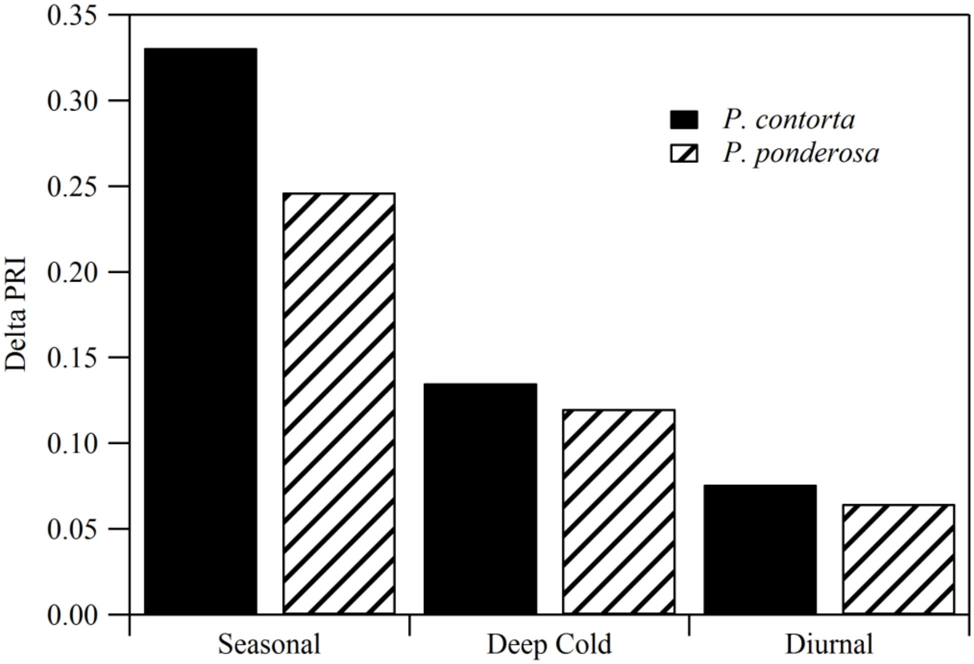

Figure 2-6. The delta PRI of *Pinus contorta* and *Pinus ponderosa* at different temporal scales. The minimum and maximum extremes for each temporal scale were selected. The seasonal PRI component was determined from the absolute values from the summer-adapted minus winter-adapted leaf PRI values. The deep cold PRI component was calculated as the deep cold (<-5 °C) minus normal winter PRI values (0 to -5 °C) obtained from different days within the same week. The diurnal PRI component was determined from the dark-state minus light-state of the leaves in the spring season where diurnal change was assumed to be largest.

Of all pigment metrics, carotenoid:chlorophyll ratios matched best with the PRI over the annual scale (Fig. 2-7a,b). Both species exhibited significant correlations between the PRI and carotenoid:chlorophyll ratios, with the *P. contorta* having slightly stronger relationships. Over this time scale, the EPS of the xanthophyll cycle and the PRI did not correlate well (Fig. 2-7c,d). In particular, during the early spring in late April (open symbols Fig. 2-7), the EPS deviated from the trend whereas the carotenoid pigment pool size did not.

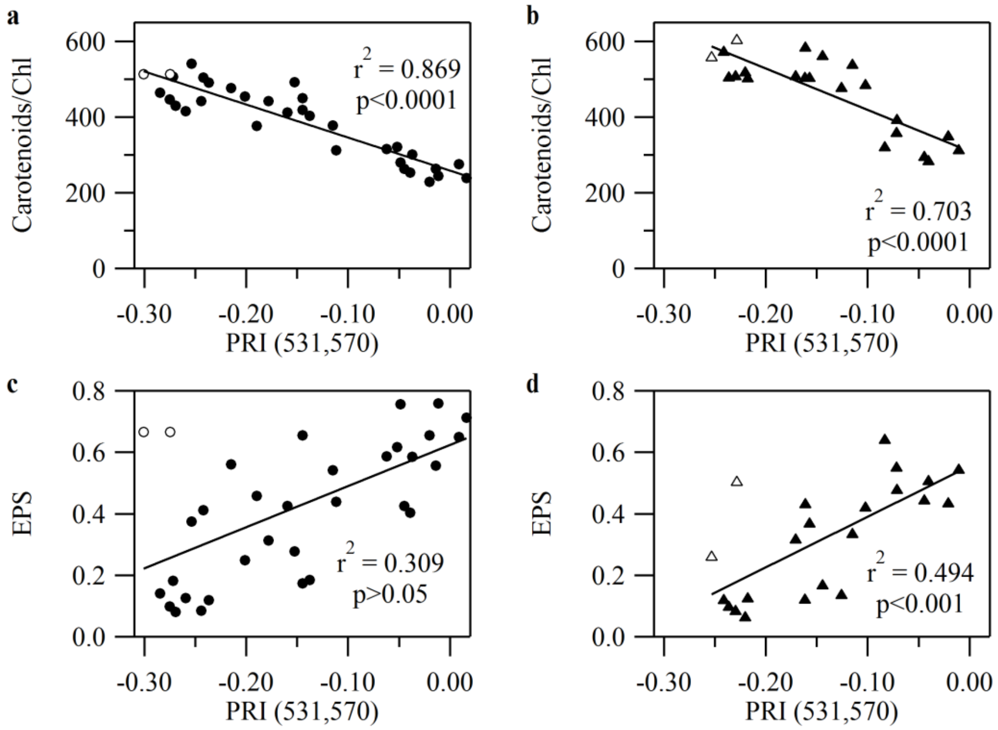

Figure 2-7. Seasonal correlation between the PRI and the total carotenoid concentration relative to chlorophyll (a,b) and EPS of the xanthophyll cycle (c,d) for *P. contorta* (left; a,c) and *P. ponderosa* (right; b,d). Data points were obtained at solar noon. Filled symbols denote all sampling dates and open symbols that denote early spring dates in late April 2013. Regression and statistics denote the correlations of all data points.

We also explored seasonal variation in the diurnal (facultative) component associated with xanthophyll cycle conversion. The diurnal response of the xanthophyll cycle and the diurnal response of the PRI exhibited similar seasonal variations for both species (Fig. 2-8). Spring, summer and autumn seasons exhibited high delta (Δ) values for both parameters indicating high diurnal variability. Largest delta values were observed during the transitional cold hardening period of the leaves in the autumn season from October to November. The winter season exhibited very low delta values near zero indicating low diurnal variability. The relationship of the seasonal ΔEPS and the ΔPRI had significant correlations for both *P. contorta* (r^2=0.769, $p<0.0001$) and *P. ponderosa* (r^2=0.691, $p<0.05$) during the stable winter and summer periods. The correlations were not significant for the whole year due to poor correlation during fall and spring transition points (*P. contorta*: r^2=0.211, $p>0.05$; *P. ponderosa*: r^2=0.000, $p>0.05$).

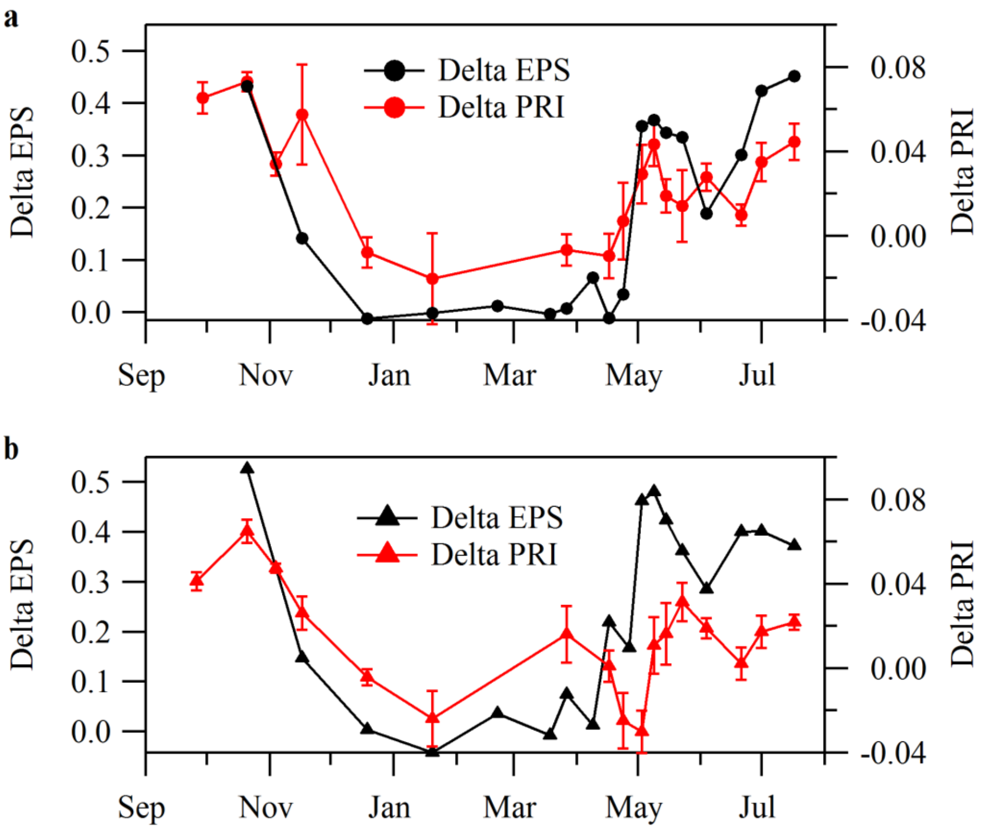

Figure 2-8. The seasonal acclimation from September 2012 to July 2013 of the diurnal response of the xanthophyll cycle (open) and the PRI (solid) for *P. contorta* (a) and *P. ponderosa* (b). Delta parameters were calculated from dark-minus light-state of the leaves on a single day. Error bars denote standard error of the mean. Since the leaves were pooled for pigment analysis, no error bars are available for Delta EPS.

Discussion

This study presents clear evidence for three distinct processes affecting the PRI in evergreen conifers: 1) a short-term, facultative response related to the operation of the xanthophyll cycle, 2) a longer-term, constitutive response related to seasonally changing carotenoid:chlorophyll ratios, and 3) a rapidly reversible response to deep cold (<-5 ºC). Both the facultative and constitutive responses have been widely reported before, but this study presents clear evidence that it is the constitutive response, and not the facultative response, that causes the primary variation in the PRI over the yearly time span. To our knowledge, the reversible deep cold response has not been reported before, and is unrelated to the xanthophyll cycle or to changes in the carotenoid:chlorophyll ratios. The three causes of the PRI variability exhibited different spectral responses, which can help identify the distinct processes. This study did not test heat and drought stress, which cause plants to respond with the conversion of the xanthophyll cycle (Demmig-Adams & Adams, 1992). In the summer, these additional stresses may induce summer downregulation that can be detected by the PRI (Sims *et al.*, 2006; Garbulsky *et al.*, 2008; Goerner *et al.*, 2009; Gamon & Bond, 2013).

The seasonal (constitutive) response of the PRI detects changes in the carotenoid:chlorophyll ratio rather than the conversion of the xanthophyll cycle, and this finding is consistent with previous reports (Stylinski *et al.*, 2002; Filella *et al.*, 2009; Garrity *et al.*, 2011; Porcar-Castell *et al.*, 2012). Like the xanthophyll cycle, an increased carotenoid:chlorophyll ratio is often associated with photoprotection due to their role in energy dissipation (Demmig-Adams &

Adams, 1996). The PRI and light-use efficiency over the long-term has seen variable correlations across vegetation stands (Goerner *et al.*, 2011). In part, this variation may be due to misinterpretations of the PRI as it can be confounded by constitutive and facultative processes along with other factors mentioned in Barton and North (2001). These experiments illustrate that the assumption of the PRI as a measure of the EPS during seasonal transitions may not be correct (Nichol *et al.*, 2000). In our study, the spring PRI values were poorly correlated with EPS (Fig. 2-7), casting doubt on the interpretation that spring PRI changes in evergreens are driven by the EPS. Instead, the weak PRI correlation with EPS during spring transition agrees with mechanistic studies of the PRI during seasonal transitions, which finds that the PRI doesn't match with the non-photochemical quenching response (Porcar-Castell *et al.*, 2012). Since the seasonal (constitutive) response of the PRI makes up most of the PRI variation, the carotenoid:chlorophyll ratio should be the considered as the primary pigment function driving the PRI signal over the long-term (weekly to seasonal).

The diurnal (facultative) response of the PRI is often associated with LUE (Gamon *et al.*, 1992; Peñuelas *et al.*, 1995; Gamon *et al.*, 1997), which is dependent on incoming irradiance and the conversion of the xanthophyll cycle. At high irradiance levels that saturate photosynthesis, the xanthophyll cycle responds to dissipate excess energy and protect the leaves from photodamage on a daily basis (Demmig-Adams, 1990). The diurnal response of the PRI was found to have a seasonal component, which was largest during transitional and growing seasons (Fig. 2-8), as also reported by Nakaji *et al.* (2006). Large variation indicates high diurnal responses of the xanthophyll cycle to changing irradiance (Demmig-Adams & Adams, 1996). We also saw high diurnal activity during the autumn cold hardening period, which could be because the xanthophyll cycle activity in combination with the changing carotenoid:chlorophyll ratios are required for energy production while transitioning to a downregulated state (Ottander *et al.*, 1995). The winter season consists of photosynthetically downregulated leaves, which have minimal diurnal variation, indicating maintenance of a high energy dissipation capacity that can efficiently dissipate all absorbed light energy. Interpretation the PRI requires consideration of pigment content and environmental context as seasonal and diurnal responses overlap.

A deep cold temperature response (<-5 °C) measured an overall decrease in albedo in the visible and near-infrared regions of the spectrum that ultimately affected the PRI. Changes in the entire spectrum suggest a change in internal light scattering within the leaf. We hypothesize that this may be due to leaf structural change; under cold winter conditions, leaves often remove water from their mesophyll tissues, preventing intracellular freezing. Ice formation within the cells of the leaves is deadly to the cells which will kill the leaf (Li & Christersson, 1993; Buchanan *et al.*, 2002; Öquist & Hüner, 2003). Dehydration may also occur during freezing and the formation of ice in intercellular spaces that may damage plant cells in a non-lethal manner (Kozlowski & Pallardy, 2002). Water removal could also increase pigment and solute concentrations within the leaves affecting spectral signals. Interestingly, the leaves survive this period of deep cold temperature and fully recovered into the spring and summer seasons. A full exploration of this phenomenon and its cause was beyond the scope of this study and further work is needed to explore potential structural and intracellular changes at deep cold temperatures that optical measurements could detect.

Reflectance spectra of conifer needles exhibited characteristic features at the PRI wavebands, 531 and 570 nm. The PRI was originally designed to use 531 nm to detect changes in the xanthophyll cycle and 570 nm as a reference due to insensitivity of that wavelength to the xanthophyll cycle (Gamon *et al.*, 1992; Gamon *et al.*, 1993; Peñuelas *et al.*, 1995; Gamon *et al.*, 1997). However, our results exhibited three types of changes that affected these wavebands to different extents. The seasonal (constitutive) response between summer and winter season had changes to both wavebands in opposite directions is likely driven by changing carotenoid:chlorophyll ratios that may amplify the absolute change resulting in the source of largest variation. The diurnal (facultative) response of the PRI wavebands between the pre-dawn and noon exhibited typical response of the varying 531 nm and a fixed reference 570 nm, consistent with previous reports (Gamon & Surfus, 1999). The subtle change at 531 nm is driven by conversion of the xanthophyll cycle that leads to a diurnal response that was the smallest source of variation in the PRI over the two-year course of this study. The deep cold response had a larger effect on the reference waveband compared to 531 nm, which was also in the same direction resulting in the second largest source of variation. These three temperature- and irradiance-based responses affected the wavebands of the PRI in unique ways that differ spectrally and kinetically. Comparing spectra or changes to the PRI wavebands, 531 and 570 nm, at different time frames can help identify some of the underlying pigment causes in the variation of the PRI. An alternative technique to partition the processes could be to re-think the PRI formulation, which was originally derived for the diurnal response, to have distinct formulas for each process, specifically for the seasonal and deep cold response.

The constitutive and facultative processes of the PRI can be utilized to detect leaf pigment responses to stresses that affect photosynthesis. The broader constitutive process can help detect season length by determining the timing of winter downregulation and spring recovery in evergreens. The finer facultative process can help detect diurnal LUE and responses to summer stress like heat and drought (Gamon & Bond, 2013). Combining the two processes, could potentially help us evaluate carbon source/sink dynamics of evergreen conifers by determining the growing season length and presence of summertime stresses that may constrain photosynthetic activity. As long as the different PRI responses and interpretation of physiological processes are considered in their correct contexts, the PRI can provide a direct approach to monitoring physiological pigment responses associated with photosynthetic activity and photoprotection.

Literature Cited

Adams WW, Demmig-Adams B, Rosenstiel TN, Brightwell AK, Ebbert V. 2002. Photosynthesis and photoprotection in overwintering plants. *Plant Biology* **4**(5): 545-557.

Barton CVM, North PRJ. 2001. Remote sensing of canopy light use efficiency using the photochemical reflectance index - Model and sensitivity analysis. *Remote Sensing of Environment* **78**(3): 264-273.

Bigras FJ, Colombo SJ. 2001. *Conifer cold hardiness*. Dordrecht: Kluwer.

Björkman O, Demmig-Adams B. 1994. Regulation of photosynthetic light energy capture, conversion, and dissipation in leaves of higher plants. In: Schulze E-D, Caldwell M eds. *Ecophysiology of Photosynthesis*: Springer Berlin Heidelberg, 17-47.

Bonan GB. 2008. Forests and climate change: Forcings, feedbacks, and the climate benefits of forests. *Science* **320**(5882): 1444-1449.

Buchanan BB, Gruissem W, Jones RL. 2002. *Biochemistry & molecular biology of plants*: John Wiley & Sons.

Butler WL. 1978. Energy distribution in photochemical apparatus of photosynthesis. *Annual Review of Plant Physiology and Plant Molecular Biology* **29**: 345-378.

Coops NC, Hilker T, Hall FG, Nichol CJ, Drolet GG. 2010. Estimation of Light-use Efficiency of Terrestrial Ecosystem from Space: A Status Report. *Bioscience* **60**(10): 788-797.

Demmig-Adams B. 1990. Carotenoids and photoprotection in plants: A role for the xanthophyll zeaxanthin. *Biochimica Et Biophysica Acta* **1020**(1): 1-24.

Demmig-Adams B, Adams WW. 1992. Photoprotection and other responses of plants to high light stress. *Annual Review of Plant Physiology and Plant Molecular Biology* **43**: 599-626.

Demmig-Adams B, Adams WW. 1996. The role of xanthophyll cycle carotenoids in the protection of photosynthesis. *Trends in Plant Science* **1**(1): 21-26.

Filella I, Amaro T, Araus JL, Peñuelas J. 1996. Relationship between photosynthetic radiation-use efficiency of Barley canopies and the photochemical reflectance index (PRI). *Physiologia Plantarum* **96**(2): 211-216.

Filella I, Peñuelas J, Llorens L, Estiarte M. 2004. Reflectance assessment of seasonal and annual changes in biomass and CO2 uptake of a Mediterranean shrubland submitted to experimental warming and drought. *Remote Sensing of Environment* **90**(3): 308-318.

Filella I, Porcar-Castell A, Munné-Bosch S, Bäck J, Garbulsky MF, Peñuelas J. 2009. PRI assessment of long-term changes in carotenoids/chlorophyll ratio and short-term changes in de-epoxidation state of the xanthophyll cycle. *International Journal of Remote Sensing* **30**(17): 4443-4455.

Gamon JA, Berry JA. 2012. Facultative and constitutive pigment effects on the Photochemical Reflectance Index (PRI) in sun and shade conifer needles. *Israel Journal of Plant Sciences* **60**(1-2): 85-95.

Gamon JA, Bond B. 2013. Effects of irradiance and photosynthetic downregulation on the photochemical reflectance index in Douglas-fir and ponderosa pine. *Remote Sensing of Environment* **135**: 141-149.

Gamon JA, Filella I, Penuelas J. 1993. The dynamic 531-nanometer delta reflectance signal: a survey of twenty angiosperm species. In: Yamamoto HY, Smith CM eds. *Photosynthetic Responses to the Environment*. Rockville: American Society of Plant Physiologists, 172-177.

Gamon JA, Peñuelas J, Field CB. 1992. A narrow waveband spectral index that tracks diurnal changes in photosynthetic efficiency. *Remote Sensing of Environment* **41**(1): 35-44.

Gamon JA, Serrano L, Surfus JS. 1997. The photochemical reflectance index: an optical indicator of photosynthetic radiation use efficiency across species, functional types, and nutrient levels. *Oecologia* **112**(4): 492-501.

Gamon JA, Surfus JS. 1999. Assessing leaf pigment content and activity with a reflectometer. *New Phytologist* **143**(1): 105-117.

Garbulsky MF, Peñuelas J, Gamon JA, Inoue Y, Filella I. 2011. The photochemical reflectance index (PRI) and the remote sensing of leaf, canopy and ecosystem radiation use efficiencies A review and meta-analysis. *Remote Sensing of Environment* **115**(2): 281-297.

Garbulsky MF, Peñuelas J, Papale D, Filella I. 2008. Remote estimation of carbon dioxide uptake by a Mediterranean forest. *Global Change Biology* **14**(12): 2860-2867.

Garrity SR, Eitel JUH, Vierling LA. 2011. Disentangling the relationships between plant pigments and the photochemical reflectance index reveals a new approach for remote estimation of carotenoid content. *Remote Sensing of Environment* **115**(2): 628-635.

Goerner A, Reichstein M, Rambal S. 2009. Tracking seasonal drought effects on ecosystem light use efficiency with satellite-based PRI in a Mediterranean forest. *Remote Sensing of Environment* **113**(5): 1101-1111.

Goerner A, Reichstein M, Tomelleri E, Hanan N, Rambal S, Papale D, Dragoni D, Schmullius C. 2011. Remote sensing of ecosystem light use efficiency with MODIS-based PRI. *Biogeosciences* **8**(1): 189-202.

Goodale CL, Apps MJ, Birdsey RA, Field CB, Heath LS, Houghton RA, Jenkins JC, Kohlmaier GH, Kurz W, Liu SR, Nabuurs GJ, Nilsson S, Shvidenko AZ. 2002. Forest carbon sinks in the Northern Hemisphere. *Ecological Applications* **12**(3): 891-899.

Grace J, Nichol C, Disney M, Lewis P, Quaife T, Bowyer P. 2007. Can we measure terrestrial photosynthesis from space directly, using spectral reflectance and fluorescence? *Global Change Biology* **13**(7): 1484-1497.

Hilker T, Coops NC, Wulder MA, Black TA, Guy RD. 2008. The use of remote sensing in light use efficiency based models of gross primary production: A review of current status and future requirements. *Science of the Total Environment* **404**(2-3): 411-423.

Horton P, Ruban AV, Walters RG. 1996. Regulation of light harvesting in green plants. *Annual Review of Plant Physiology and Plant Molecular Biology* **47**: 655-684.

Hüner NPA, Öquist G, Hurry VM, Krol M, Falk S, Griffith M. 1993. Photosynthesis, photoinhibition and low temperature acclimation in cold tolerant plants. *Photosynthesis Research* **37**(1): 19-39.

Hüner NPA, Öquist G, Sarhan F. 1998. Energy balance and acclimation to light and cold. *Trends in Plant Science* **3**(6): 224-230.

Kozlowski TT, Pallardy SG. 2002. Acclimation and adaptive responses of woody plants to environmental stresses. *Botanical Review* **68**(2): 270-334.

Levitt J. 1980. *Responses of plants to environmental stresses*. New York: Academic Press.

Li PH, Christersson L. 1993. *Advances in plant cold hardiness*: CRC Press.

Nakaji T, Oguma H, Fujinuma Y. 2006. Seasonal changes in the relationship between photochemical reflectance index and photosynthetic light use efficiency of Japanese larch needles. *International Journal of Remote Sensing* **27**(3): 493-509.

Nichol CJ, Huemmrich KF, Black TA, Jarvis PG, Walthall CL, Grace J, Hall FG. 2000. Remote sensing of photosynthetic-light-use efficiency of boreal forest. *Agricultural and Forest Meteorology* **101**(2-3): 131-142.

Öquist G, Hüner NPA. 2003. Photosynthesis of overwintering evergreen plants. *Annual Review of Plant Biology* **54**: 329-355.

Osmond CB. 1981. Photo-respiration and photoinhibition Some implications for the energetics of photosynthesis. *Biochimica Et Biophysica Acta* **639**(2): 77-98.

Ottander C, Campbell D, Öquist G. 1995. Seasonal changes in photosystem II organization and pigment composition in *Pinus sylvestris*. *Planta* **197**(1): 176-183.

Pan YD, Birdsey RA, Fang JY, Houghton R, Kauppi PE, Kurz WA, Phillips OL, Shvidenko A, Lewis SL, Canadell JG, Ciais P, Jackson RB, Pacala SW, McGuire AD, Piao SL, Rautiainen A, Sitch S, Hayes D. 2011. A Large and Persistent Carbon Sink in the World's Forests. *Science* **333**(6045): 988-993.

Peñuelas J, Filella I, Gamon JA. 1995. Assessment of photosynthetic radiation-use efficiency with spectral reflectance. *New Phytologist* **131**(3): 291-296.

Porcar-Castell A, Garcia-Plazaola JI, Nichol CJ, Kolari P, Olascoaga B, Kuusinen N, Fernandez-Marín B, Pulkkinen M, Juurola E, Nikinmaa E. 2012. Physiology of the seasonal relationship between the photochemical reflectance index and photosynthetic light use efficiency. *Oecologia* **170**(2): 313-323.

Rahman AF, Gamon JA, Fuentes DA, Roberts DA, Prentiss D. 2001. Modeling spatially distributed ecosystem flux of boreal forest using hyperspectral indices from AVIRIS imagery. *Journal of Geophysical Research-Atmospheres* **106**(D24): 33579-33591.

Sims DA, Gamon JA. 2002. Relationships between leaf pigment content and spectral reflectance across a wide range of species, leaf structures and developmental stages. *Remote Sensing of Environment* **81**(2-3): 337-354.

Sims DA, Luo HY, Hastings S, Oechel WC, Rahman AF, Gamon JA. 2006. Parallel adjustments in vegetation greenness and ecosystem CO2 exchange in response to drought in a Southern California chaparral ecosystem. *Remote Sensing of Environment* **103**(3): 289-303.

Stylinski CD, Gamon JA, Oechel WC. 2002. Seasonal patterns of reflectance indices, carotenoid pigments and photosynthesis of evergreen chaparral species. *Oecologia* **131**(3): 366-374.

Thayer SS, Björkman O. 1990. Leaf xanthophyll content and composition in sun and shade determined by HPLC. *Photosynthesis Research* **23**(3): 331-343.

Vogg G, Heim R, Hansen J, Schäfer C, Beck E. 1998. Frost hardening and photosynthetic performance of Scots pine (*Pinus sylvestris* L.) needles. I. Seasonal changes in the photosynthetic apparatus and its function. *Planta* **204**(2): 193-200.

Chapter 3. Parallel Seasonal Transition of Photosynthesis and Optical Properties for Conifer Needles

Introduction

Boreal forests cover about 1135 Mha in the northern hemisphere and stores about 32% of the total carbon stock of established forests (Pan *et al.*, 2011). These boreal forests are dominated by evergreen conifers that have acted as a net carbon sink for the removal of CO_2 from the atmosphere (Apps *et al.*, 1993; Ciais *et al.*, 1995). However, the boreal region has been undergoing significant climate change including increases in temperature (IPCC, 2007). Recent studies have suggested reduced carbon uptake under warmer conditions (Canadell *et al.*, 2007; Le Quéré *et al.*, 2009). Increased disturbances and environmental stresses can lead to interannual variability, and can cause the boreal forests to become a net carbon source (Kurz & Apps, 1999; Goodale *et al.*, 2002; Kurz *et al.*, 2008). Consequently, the role of the boreal forest as a carbon sink is now highly uncertain (Thurner *et al.*, 2014).

The effects of climate change on the boreal forest are difficult to predict, in part due to the survival strategy of evergreens that undergo strong seasonality in their photosynthetic and respiratory activity. Evergreens are photosynthetically active in the short summer season and are photosynthetically inactive (downregulated) during the longer winter season. Evergreen photosynthetic activity is affected by photoperiod and temperatures that signal the evergreens to acclimate for long-term survival (Bigras & Colombo, 2001). The autumn and spring seasons are transitional periods where the plants undergo cold hardening and spring recovery, respectively (Vogg *et al.*, 1998). Seasonal timing affects the role of evergreens in the global carbon cycle as climate change can affect season length and shift the onset of the cold hardening and spring recovery periods (Ensminger *et al.*, 2004).

Cold winter temperatures results in the downregulation of photosynthesis which leads to a potential imbalance of light energy capture and usage. Over-excitation of photosystems leads to permanent photodamage to the photosynthetic apparatus that impairs the leaves' ability to photosynthesize (Powles, 1984). To prevent photodamage in the winter, evergreen leaves undergo cold hardening signaled by reduced photoperiod and decreasing temperatures (Levitt, 1980; Vogg *et al.*, 1998; Bigras & Colombo, 2001). Photoprotective processes involve changes at the pigment level which allows the leaves to dissipate excess energy via thermal dissipation to maintain an energy balance (Butler, 1978; Baker, 2008; Verhoeven, 2014). Cold hardening results in the rearrangement of pigments (Ottander *et al.*, 1995) and an increase of carotenoid pigment pool size (Björkman & Demmig-Adams, 1994; Demmig-Adams & Adams, 1996; Verhoeven *et al.*, 1999). Dehardening of evergreens and the spring recovery of photosynthesis involves reversal of the pigment changes which starts in spring signaled by warmer temperatures and longer photoperiod (Ottander *et al.*, 1995; Vogg *et al.*, 1998).

Monitoring spring recovery could provide a crucial indicator of growing season length and overall carbon balance. Previous work examining the spring recovery of pigments and proteins (Verhoeven *et al.*, 1996; Ensminger *et al.*, 2004), chlorophyll fluorescence (Porcar-Castell, 2011) and light-use efficiency (Nichol *et al.*, 2002; Porcar-Castell *et al.*, 2012) have all exhibited a rapid spring reactivation. More work is needed to compare the different methods monitoring photosynthetic activity as a way to understand shifting seasonal activation.

In this study, we followed the seasonal processes over the course of a year in boreal climate ranging from daily mean temperatures of -30 °C to +30 °C. The particular purpose of this study was to monitor the spring activation of photosynthesis by following a variety of physiological parameters at the leaf level. We also examined the kinetics of the different parameters over the course of spring recovery, allowing a better understanding of the timing and mechanisms of the photosynthetic activation processes.

Materials and Methods

Two conifer species Lodgepole pine (*Pinus contorta* D.) and Ponderosa pine (*Pinus ponderosa* Laws.), were grown outdoors at the University of Alberta, Canada. During the summer of 2010, one year old seedlings were planted in a 1:2 soil mixture of sandy top soil and sunshine mix (Sunshine Mix 4, Sun Gro Horticulture, Agawam, MA, USA) with added slow release fertilizer (Nutricote 14-14-14, Sun Gro Horticulture, Agawam, MA, USA). They were initially potted in small 2.31 L pots (CP412CH, Stuewe & Sons, Tangent, OR, USA) for their long-term acclimation. To maintain an adequate rooting volume and avoid water or nutrient stress, these plants were repotted in the summer of 2011 into medium 2.83 L (TP414, Stuewe & Sons, Tangent, OR, USA) and in the summer of 2012 into large 6.23 L pots (TP616, Stuewe & Sons, Tangent, OR, USA). The pots were arranged by species in rectangular plots 1.5 m x 1.5 m to simulate two homogenous forest stands experiencing natural light and temperature conditions across the different seasons. The plants were watered daily throughout the non-freezing period to avoid water stress. During winter, extra pots of soil and a plywood frame were added to the outside edges of the plots, and a 3 cm layer of peat moss was added to the soil surface of all pots to provide additional insulation to the roots during the cold winter.

A weather station provided photosynthetic photon flux density (PPFD) (S-LIB-M003, Onset, Bourne, MA, USA) and air temperature (S-THB-M002, Onset, Bourne, MA, USA) that were collected every minute on a datalogger (U30-NRC, Onset, Bourne, MA, USA). The weather data were aggregated into 15 minute averages that were later expressed as daily averages with a 5-day running mean. The sensors were set up at the same height as the canopy and located within 3-5 m to provide representative conditions incoming PPFD and ambient temperatures experienced by the leaves.

The seasonal acclimation of photosynthetic parameters was monitored for both evergreen species from June 2012 to July 2013. They were measured every other week from June 2012 to February 2013 and on a weekly basis from March 2013 to July 2013. Data collection from 12:00 to 14:00 (within 1-2 hours of solar noon) was to ensure the presence of maximum sunlight and reduce diurnal variability. Six randomly chosen plants were monitored for the duration of the study. All measurements from a single day were averaged together to follow the seasonal dynamics. Youngest fully developed needles from the 2012 cohort at the top of the canopy were used throughout the experiment to keep growth light conditions consistently high and to avoid interference of shading effects of different elevations within a canopy.

Optical Sampling

A spectrometer (UniSpec-SC, PP Systems, Amesbury, MA, USA) operated using a palmtop PC (1000CX, Hewlett-Packard Company, Palo Alto, CA, USA) equipped with a bifurcated fibre optic (UNI410, PP Systems, Amesbury, MA, USA) was used to measure spectral reflectance. A needle leaf clip (UNI501, PP Systems, Amesbury, MA, USA) was utilized to hold the fibre tip at a fixed angle and position relative to the leaf surface to ensure repeatable technique and enable reflectance sampling of individual needles (0.6 mm diameter spot size). Each leaf measurement was preceded by a dark measurement and white reference scan (Spectralon, Labsphere, North Sutton, NH, USA), and reflectance was calculated from each leaf scan divided by a white reference scan after correction for dark current. The integration time was set to 50 ms and 10 successive scans were automatically averaged for each measurement. The PRI was calculated as:

$$PRI = \frac{R_{531} - R_{570}}{R_{531} + R_{570}} \tag{1}$$

R indicates reflectance, and the subscript indicates the waveband in nm. For each plant, 5 different leaves were measured providing a total of 30 samples per species. All measurements from the same sampling day were combined into a single average value.

Pigment Assay

Leaves were removed from the plants and immediately cut into three 1 cm long segments, measured for leaf area, stored in liquid nitrogen, and later transferred to an 80 °C freezer for long-term storage. Batches of 6 leaf samples from a given date and time were pooled together for pigment analysis using high-performance liquid chromatography (HPLC) (1260 Infinity, Agilent Technologies, Santa Clara, CA, USA). HPLC sampling following the Thayer and Björkman (1990) method to find the pigment concentrations of various carotenoid and chlorophyll pigments. The HPLC system was calibrated using pigment standards from DHI (DHI LAB Products, Hørsholm, Denmark).

The carotenoid:chlorophyll ratio was measured as the ratio of all carotenoids including neoxanthin, violaxanthin, antheraxanthin, lutein, zeaxanthin and β-carotene to the total concentration of chlorophyll a and b (mmol mol^{-1}). The xanthophyll cycle composition was determined as the epoxidation state (EPS) which was expressed as:

$$EPS = \frac{V + 0.5A}{V + A + Z} \tag{2}$$

The EPS is an expression of the non-photoprotective ratio of the xanthophyll cycle. The letters indicate absolute concentration (µmol m^{-2}) of each xanthophyll pigment violaxanthin (V), antheraxanthin (A) and zeaxanthin (Z).

Chlorophyll Fluorescence

Chlorophyll fluorescence was monitored using the portable Mini-PAM Fluorometer (Walz, Effeltrich, Germany). The fluorometer was fitted with a fibre optic and leaf clip (Walz, Effeltrich, Germany) which kept the fibre tip at a fixed angle and position for repeatability. Leaves were carefully bundled together and clamped within the leaf clip holder while minimizing the positional change of the leaves to sunlight. The leaf clip had a built in quantum sensor that detected the leaves incoming PPFD. The fluorescence, F, was monitored to ensure that the leaves were stable prior to sampling. For data collection under natural light conditions, a short 0.8 s pulse of saturating light of approximately 3000 µmol photons m^{-2} s^{-1} was provided and the maximal fluorescence, Fm', was obtained. The fluorometer calculated the fluorescence yield parameter which is indicative of photosynthetic efficiency of Photosystem II (Baker, 2008).

$$Yield = \varphi = \frac{\Delta F}{Fm'} \tag{3}$$

A linear correlation between yield and PPFD was calculated and the maximum yield was estimated at 1500 µmol m^{-2} s^{-1}. Utilizing the yield parameter and the measured PPFD allowed for the calculation of the relative electron transport rate (ETR) (µmol m^{-2} s^{-1}). This parameter provided a more direct estimation related to photosynthetic activity (Maxwell & Johnson, 2000; Baker, 2008).

$$ETR = \varphi \times PPFD \times 0.5 \times \frac{APAR}{PAR} \tag{4}$$

The PPFD was obtained from the built-in quantum sensor from the leaf clip. The fraction of absorbed light (APAR) was obtained from the spectral reflectance measurements. APAR is the sum of light absorbance from 400 to 700 nm and the PAR is the total energy from wavebands 400 to 700 nm. The fraction of absorbed light differs between species and changes seasonally so by incorporating a flexible value, the fluorescence based estimation was corrected for relative light absorption (Maxwell & Johnson, 2000). A light curve of ETR was calculated and the maximum ETR was estimated at 1500 µmol m^{-2} s^{-1}. For each species, measurements from 3 leaf bundles were collected per plant, providing a sample size of about 18 for each species.

Gas Exchange

Photosynthesis was measured using the Li-6400XT portable photosynthesis system (LICOR, Lincoln, Nebraska, USA). Six leaves from an individual plant were placed inside the gas exchange chamber and a photosynthetic light response curve was then measured. The light curve was set to monitor light intensity values of 1500, 1000, 800, 600, 400, 100, 50 and 0 µmol photons m^{-2} s^{-1}. For each stage, there was a 1-minute minimum and 3-minute acclimation time before measurement and changing to the next light level. The chamber environmental settings were set to match current ambient temperatures and the reference CO_2 was set to 395 µmol mol^{-1} which is approximately the same as atmospheric levels. Air flow was set to 400 µmol s^{-1}. Five plants were measured for each species over the course of spring recovery from March 2013 to July 2013 on a weekly basis. After averaging the photosynthetic light response curves together, the LUE on an incident light basis was calculated based on the initial slope at low light intensities and the maximum photosynthetic rate (μmol CO_2 m^{-2} s^{-1}) was at 1500 μmol m^{-2} s^{-1} (near the saturating region of the curve).

Kinetics

All the methods incorporated in this project provided indicators of the 2013 spring recovery. To examine the kinetics of spring recovery, data ranging from 8 March 2013 to 17 July 2013 were selected, which incorporate winter-, spring- and summer-adapted states. For comparative purposes, the values of all the parameters were normalized from zero to one. A sigmoidal fit incorporating stable winter and summer days and transitional spring recovery was estimated using commercial plotting software (Igor Pro, WaveMetrics, Portland, OR, USA). To compare the timing of the photosynthetic spring recovery, the half-point of the recovery was also estimated with a 95% confidence interval.

Results

Daily mean temperature and PPFD exhibited large seasonal changes (Fig. 3-1). Based on temperature, there were four distinct seasons that likely affected the growth conditions of the plants over the year. The daily mean temperatures in the summer, from June to August, were typically above 18 °C and consisted of high PPFD due to long photoperiod and high sun angle. During the autumn season, from September to November, both daily mean temperature and PPFD declined gradually. The winter season, from December to March, had daily mean temperatures below 0 °C and low PPFD due to short photoperiod and low sun angle. The spring season in April and May had rapid recovery of daily mean temperature. PPFD recovery exhibited slight uncoupling with temperature starting the recovery earlier in February and gradually increased until May.

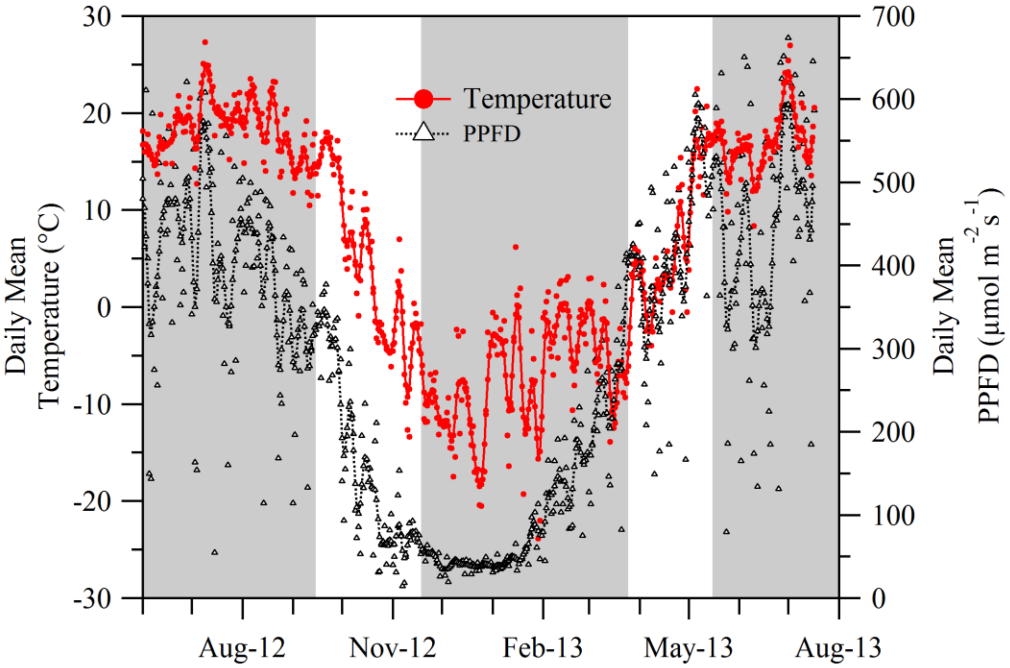

Figure 3-1. Seasonal dynamics of daily mean temperature and PPFD with 5-day running means over one year in Edmonton, AB. Grey regions denote summer and winter, and white regions denote transitional autumn and spring seasons.

The PRI exhibited seasonal variability for both species roughly in parallel with temperature (Fig. 3-2). Maximum values around -0.03 were observed in the summer from June to August. In the autumn from September to November, the PRI gradually decreased. During the early winter, from December to January, deep cold temperatures resulted in an abrupt increase in the PRI. The remainder of the winter season had minimum values around -0.27 and -0.23 for *P. contorta* and *P. ponderosa*, respectively. The lowest PRI values were observed in late April. In the spring, May, the PRI rapidly increased from the minimum winter values to the maximum summer values within 4 weeks.

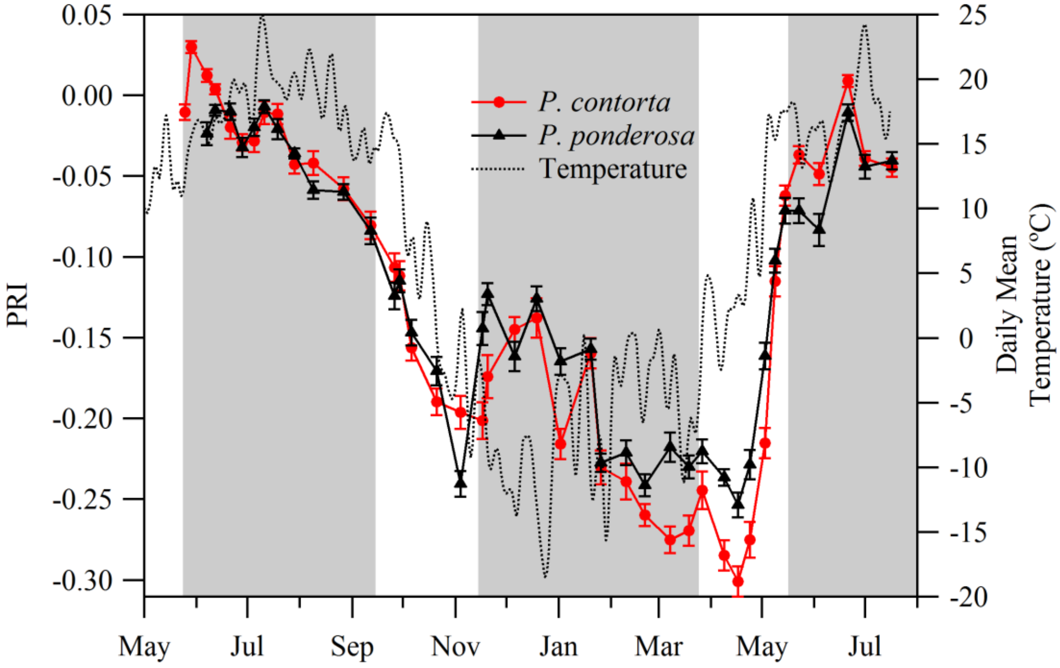

Figure 3-2. The annual dynamics of the PRI for *P. contorta* and *P. ponderosa* from May 2012 to July 2013. Error bars denote the standard error of the mean (n = 30). The 5-day running mean of temperature shows annual temperature trends. Grey regions denote summer and winter, and white regions denote transitional autumn and spring seasons.

The photosynthetic pigments exhibited seasonal changes in composition and pool size. The EPS of the xanthophyll cycle pigments followed the temperature trend and in the autumn gradually decreased from September to November (Fig. 3-3a). Lowest EPS levels were exhibited in the winter season indicative of high relative zeaxanthin content (photoprotective state). The absolute lowest EPS however occurred in late April, just before the start of the spring recovery of temperature. Spring recovery of the EPS occurred within about a week as it increased by over fivefold from around 0.10 to >0.50 (Fig. 3-3a). The carotenoid:chlorophyll ratio exhibited seasonal changes mirroring the temperature trends (Fig. 3-3b). This ratio gradually increased from September to November, reaching highest levels in the winter, by about twofold higher than the summer levels. The highest carotenoid:chlorophyll ratios occurred with a small peak in late April/early May just before spring recovery, when a rapid decline in the ratios occurred.

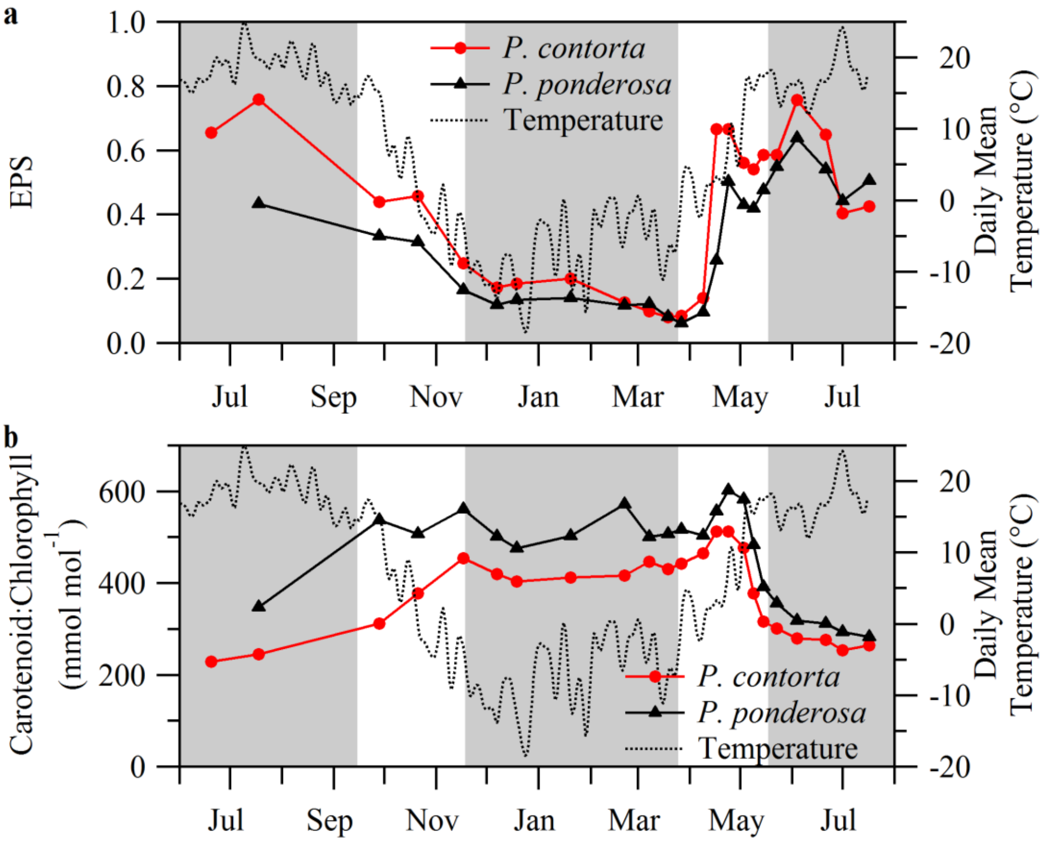

Figure 3-3. Seasonal dynamics of pigments in *P. contorta* and *P. ponderosa* from June 2012 to July 2013. The EPS of the xanthophyll cycle (a) and the carotenoid:chlorophyll ratios (b). The 5-day running mean of temperature shows annual temperature trends. Since the leaves were pooled for pigment analysis, no error bars are available (n = 6). Grey regions denote summer and winter, and white regions denote transitional autumn and spring seasons.

Chlorophyll fluorescence parameters exhibited seasonal variation in both pine species. Fluorescence yield (Fig. 3-4a) and electron transport rate (Fig. 3-4b) had similar patterns roughly in parallel with seasonal temperature trends. Highest values were observed in the summer around fluorescence yield around 0.5, and ETR around 300 µmol m^{-2}s^{-1}, and these values declined from October to November. During early winter around -10 °C in December and parts of January, fluorescence yield and ETR values dropped to zero indicating complete downregulation. When winter temperatures slightly increased near 0 °C, we observed a slight increase in activity. Spring recovery occurred from mid-April to early-May over about 4 weeks.

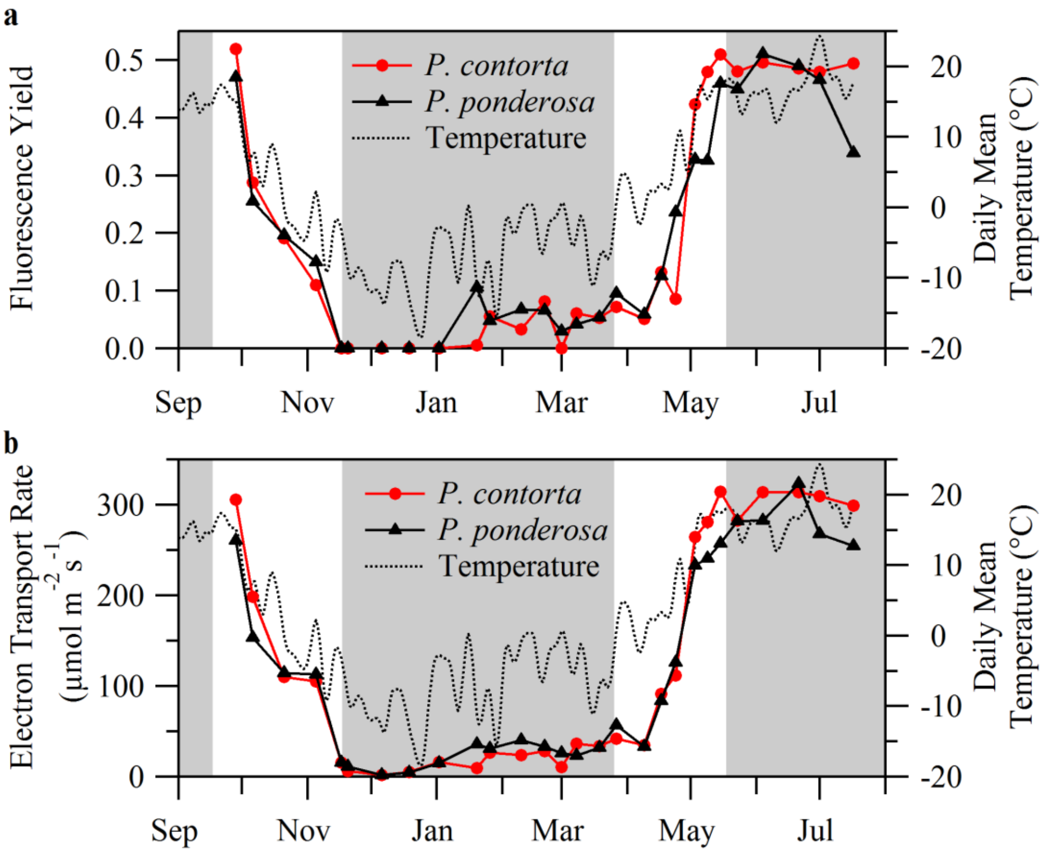

Figure 3-4. Seasonal dynamics of chlorophyll fluorescence derived parameters in *P. contorta* and *P. ponderosa* from September 2012 to July 2013. The fluorescence yield (a) and electron transport rate (b) (n = 18). The 5-day running mean of temperature shows annual temperature trends. Grey regions denote summer and winter, and white regions denote transitional autumn and spring seasons.

Correlations between photosynthetic parameters are shown in Table 3-1a (*P. contorta*) and Table 3-1b (*P. ponderosa*). Deep cold days (<-5 °C) were removed from the correlations due to decoupling in the PRI response (note that this deep-cold PRI response was discussed in Chapter 2). The PRI had significant correlations with fluorescence yield, ETR, and carotenoid:chlorophyll ratios, which had similar r^2 for *P. ponderosa* whereas for *P. contorta* it was strongest with carotenoid:chlorophyll ratios. EPS and carotenoid:chlorophyll ratios showed the lowest correlations (*P. contorta*: 0.185; *P. ponderosa*: 0.377). In *P. contorta*, EPS had weak correlations with all parameters (Table 3-1a). In *P. ponderosa*, the EPS had weak correlation with the PRI and stronger correlations with fluorescence yield and ETR (Table 3-1b).

Table 3-1a. The annual linear correlation of key parameters for *Pinus contorta.*
* P < 0.05; ** P < 0.01; *** P < 0.001; **** P < 0.0001

r^2	PRI	Yield	ETR	EPS	Carotenoids:Chl
PRI	1				
Yield	0.760****	1			
ETR	0.762****	0.982****	1		
EPS	0.357**	0.420**	0.500**	1	
Carotenoids:Chl	0.896****	0.647****	0.608***	0.185	1

Table 3-1b. The annual linear correlation of key parameters for *Pinus ponderosa*.
* P < 0.05; ** P < 0.01; *** P < 0.001; **** P < 0.0001

r^2	PRI	Yield	ETR	EPS	Carotenoids:Chl
PRI	1				
Yield	0.675****	1			
ETR	0.728****	0.967****	1		
EPS	0.562***	0.783****	0.803****	1	
Carotenoids:Chl	0.707****	0.451**	0.471**	0.377**	1

Gas exchange provided a direct measurement of photosynthesis during the course of spring recovery. Both light-use efficiency (Fig. 3-5a) and maximum photosynthetic rate (Fig. 3-5b) displayed similar patterns roughly in parallel with increasing temperature. Both parameters during the late winter in March had values around zero exhibiting the photosynthetically downregulated state of the plants. Spring recovery initiated in mid-April and fully completed by mid-May for LUE and late-May for maximum photosynthetic rate. Stable summer values around 0.04 LUE and about 15 µmol CO_2 $m^{-2}s^{-1}$ were retained for the remainder of the observation period (Fig. 3-5).

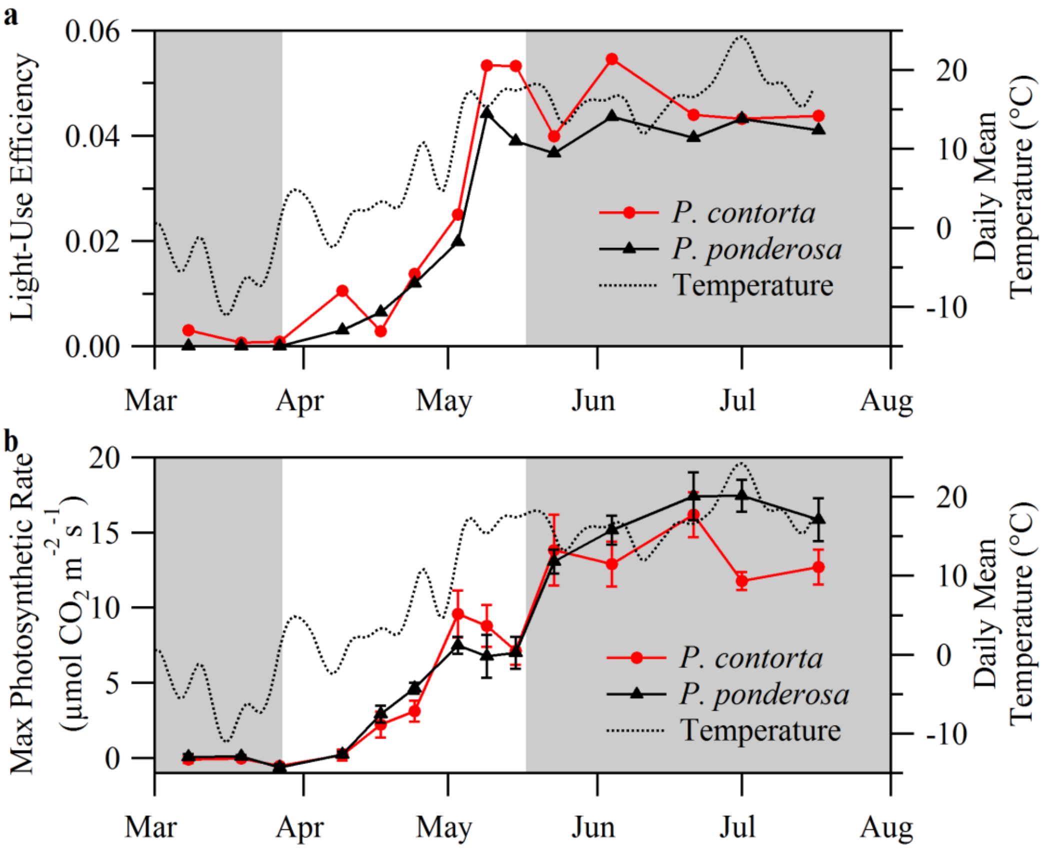

Figure 3-5. The 2013 Spring recovery of photosynthesis in *P. contorta* and *P. ponderosa* measured with a gas exchange system. The light-use efficiency (a) and maximum photosynthetic rate (b) (n = 6). The 5-day running mean of temperature shows spring recovery temperature trends. Error bars denote standard error of the mean. Grey regions denote summer and winter, and white regions denote transitional autumn and spring seasons.

A sigmoidal fit was applied to all parameters during the spring recovery to evaluate timing and kinetics (Fig. 3-6). All parameters exhibited large changes over the winter to summer transition. Data points up to day 90 represent stable winter-adapted states of the leaves. Intermediate values indicate spring transition of the leaves. Stable summer-adapted leaves exhibit the full recovery of the parameters.

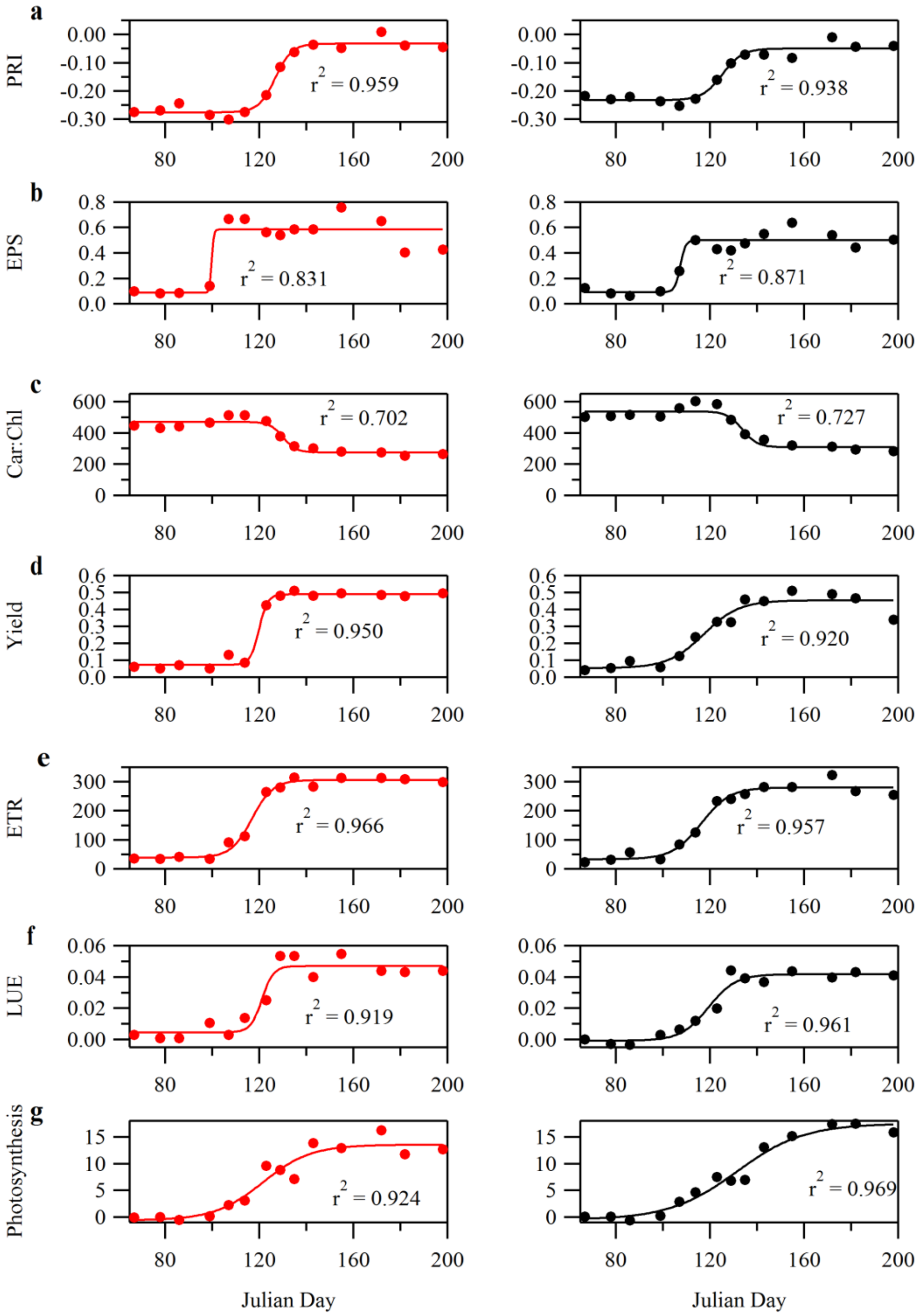

Figure 3-6. Sigmoidal fits for all parameters during the 2013 spring recovery for *P. contorta* (red) and *P. ponderosa* (black). The metrics include PRI (a), EPS (b), carotenoid:chlorophyll ratios (c), yield (d), ETR (e), LUE (f) and photosynthesis (g). $P<0.05$.

The spring recovery in 2013 occurred rapidly during April and May as temperature and PPFD levels increased (Fig. 3-1). Each photosynthetic parameter exhibited different kinetics, measured as speed of recovery and timing of the half recovery values for both species (Fig. 3-6; Table 3-2). EPS recovered abruptly in mid-April, showing only one transitional point. ETR, fluorescence yield and LUE responded a bit more slowly at the end of April. Maximum photosynthetic rate recovered the most gradually, with a half value at the beginning of May for *P. contorta* and mid-May for *P. ponderosa*. The PRI followed these parameters closely recovering early- to mid-May (note that the PRI was slightly behind photosynthesis for *P. contorta*, and ahead for *P. ponderosa*). The carotenoids:chlorophyll ratios (inverted to display similar shape of spring recovery) closely followed the PRI, with a half value at mid-May. The order and rate of spring recovery for each parameter can be more clearly seen in Figure 3-7, which overlays the sigmoidal fits for a better visual comparison of the responses shown in Figure 3-6. Comparing the species, *P. contorta* exhibited an earlier recovery compared to *P. ponderosa* (Table 3-2).

Table 3-2. The half recovery times in Julian days for the sigmoid fit of photosynthetic parameters during the 2013 spring recovery for *P. contorta* and *P. ponderosa*. 95% confidence interval. (note that these are arranged in order of recovery for *P. contorta*)

	P. contorta	*P. ponderosa*
EPS	99.883 ± 6.22	107.43 ± 8.16
ETR	116.98 ± 2.18	116.39 ± 3.85
Yield	119.95 ± 2.59	117.44 ± 7.03
LUE	121.24 ± 5.02	119.41 ± 4.70
Photosynthesis	121.55 ± 9.20	131.49 ± 7.22
PRI	126.89 ± 2.39	125.33 ± 3.72
Chlorophyll:Carotenoids	130.14 ± 3.73	133.78 ± 4.48

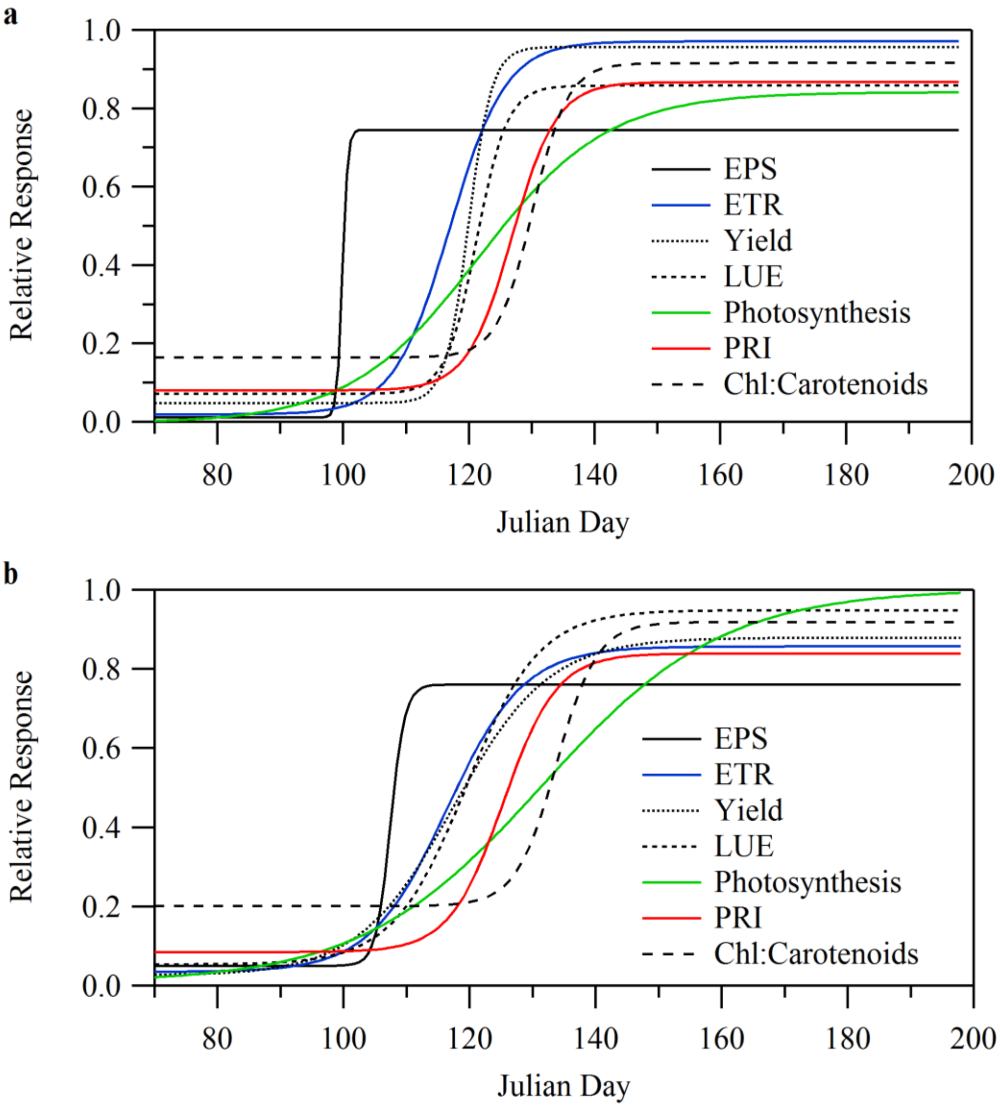

Figure 3-7. Overlaid sigmoidal fits (from Fig. 3-6), showing the relative response of photosynthetic parameters during the 2013 spring recovery for *P. contorta* (a) and *P. ponderosa* (b). The dates range from the late winter in March to the summer in July.

The linear correlations of all parameters during spring recovery exhibited stronger relationships compared to the annual correlations for both *P. contorta* (Table 3-3a) and *P. ponderosa* (Table 3-3b). The PRI was significantly correlated with all parameters and was weakest with EPS. Chlorophyll fluorescence parameters, yield and ETR, had strongest correlations with LUE and weakest with

EPS in *P. contorta* (Table 3-3a) and Carotenoid:Chl in *P. ponderosa* (Table 3-3b). Most notably, photosynthesis had significant correlations with all parameters and was weakest with EPS in *P. contorta* (Table 3-3a).

Table 3-3a. The linear correlation of key parameters for *P. contorta* and spring recovery. * $P < 0.05$; ** $P < 0.01$; *** $P < 0.001$; **** $P < 0.0001$

r^2	PRI	Yield	ETR	EPS	Car:Chl	LUE	Photo-synthesis
PRI	1						
Yield	0.849****	1					
ETR	0.833****	0.980****	1				
EPS	0.275*	0.441**	0.530**	1			
Car:Chl	0.895****	0.639***	0.597***	0.083	1		
LUE	0.828****	0.907****	0.912****	0.439**	0.638***	1	
Photo-synthesis	0.844****	0.867****	0.888****	0.488**	0.628***	0.757 ****	1

Table 3-3b. The linear correlation of key parameters for *P. ponderosa* and spring recovery. $P < 0.05$; ** $P < 0.01$; *** $P < 0.001$; **** $P < 0.0001$

r^2	PRI	Yield	ETR	EPS	Car:Chl	LUE	Photo-synthesis
PRI	1						
Yield	0.829****	1					
ETR	0.873****	0.958****	1				
EPS	0.620***	0.859****	0.846****	1			
Car:Chl	0.792****	0.548**	0.531**	0.353*	1		
LUE	0.878****	0.882****	0.911****	0.777****	0.608***	1	
Photo-synthesis	0.847****	0.822****	0.845****	0.741****	0.725****	0.800****	1

Discussion

The spring recovery of photosynthesis in evergreen conifers is a complex process involving several mechanisms that differ in kinetics. Variations between the parameters leading to low correlations were likely due to differences in component processes that decouple during the spring recovery (Porcar-Castell *et al.*, 2012). EPS recovered the earliest suggesting that the reactivation of the xanthophyll cycle occurs first. Chlorophyll fluorescence and LUE recovered next indicating that the photosystem II was next to become active. The slowest parameters to recover were the PRI and carotenoid:chlorophyll ratios likely due to the energy and time constraints of producing chlorophyll and degradation of carotenoid concentrations. Gas exchange recovered the most gradually, and only fully recovered once all other parameters had done so. These findings show that a combination of parameters associated with photosynthesis recovers with different kinetics, and contribute to the overall rate of gas exchange. Kinetics between species also differed slighty (*P. contorta* tending to recover sooner than *P. ponderosa*), which may have implications for the activation of photosynthesis and growing season length (Verhoeven, 2013).

Leaf pigments exhibited at least two seasonal responses that could be associated with photoprotection. Cold hardening in the autumn included changes in the xanthophyll cycle composition, as measured by the EPS, which would increase the potential for photoprotection (Demmig-Adams & Adams, 1996; Horton *et al.*, 1996; Verhoeven *et al.*, 1996; Hüner *et al.*, 1998; Verhoeven *et al.*, 1999; Öquist & Hüner, 2003). EPS changes are typically associated with rapid adjustments of the xanthophyll cycle, and can be considered a facultative response (Gamon & Berry, 2012). Carotenoid:chlorophyll ratios also increased during cold hardening, which could further benefit photoprotection with increased concentrations of carotenoids and loss of chlorophyll, which could enhance energy dissipation and decrease light absorption (Ottander *et al.*, 1995; Demmig-Adams & Adams, 1996; Vogg *et al.*, 1998; Gilmore & Ball, 2000; Adams *et al.*, 2002; Adams *et al.*, 2004). Carotenoid:chlorophyll ratios are slowly changing adjustments representing a more constitutive response (Gamon & Berry, 2012). During the spring recovery, these overwintering pigment responses reversed, lowering potential photoprotection with the onset of photosynthesis.

Our results demonstrated that seasonally changing PRI was more strongly correlated with gradually changing carotenoid:chlorophyll ratios than with EPS, whether evaluated annually or during spring recovery, which is consistent with previous reports indicating a strong role for pigment pool sizes in seasonal PRI patterns (Stylinski *et al.*, 2002; Filella *et al.*, 2009; Garrity *et al.*, 2011; Porcar-Castell *et al.*, 2012). While this study did not clarify the exact functional role of these two seasonal pigment changes, the stronger correlation of the PRI with carotenoid:chlorophyll ratios indicate that these ratios and not EPS were primarily driving the spring transitions in the PRI. The assumption that the PRI detects EPS and LUE during spring transitions for boreal forests may not be entirely correct (Nichol *et al.*, 2000), and the poor link between the PRI and EPS seen here seems consistent with the poor relationships between the PRI and non-photochemical quenching (Porcar-Castell *et al.*, 2012). The PRI has multiple responses to different environmental stresses and its interpretation needs to consider the temporal context to differentiate the constitutive and facultative processes.

The PRI and chlorophyll fluorescence measurements can act as proxies of photosynthesis over seasonal transition periods. Remote sensing provides a tool to measure photosynthetic activity at the ecosystem level utilizing parameters like the PRI (Sims & Gamon, 2002; Gamon & Berry, 2012; Porcar-Castell *et al.*, 2012) and solar-induced fluorescence (Meroni *et al.*, 2009; Frankenberg *et al.*, 2011). These parameters provide a direct approach for estimating photosynthetic activity by detecting physiological responses to stress. Variations may arise when monitoring at the ecosystem level caused from background material, heterogeneity, canopy structure and varying illumination (Barton & North, 2001). Our study was performed at the leaf level, so large scale interpretation remains unresolved (however, see the next chapter). Despite these challenges, the PRI and chlorophyll fluorescence detects parallel patterns associated with photosynthetic activity, but large scale methods still need to consider their mechanistic interpretation in light of the work shown here.

Understanding the seasonal patterns of photosynthesis and how different parameters respond during spring recovery can help evaluate changing growing season length in evergreens. This study demonstrated that the PRI can detect photosynthetic activity, since both exhibited similar responsiveness to winter downregulation and spring recovery. The long-term (constitutive) response of the PRI driven primarily by carotenoid:chlorophyll ratios could help develop photosynthesis models that utilize this association with photosynthetic activity. Detecting the downregulation and recovery of photosynthesis can provide a measure of growing season length, which is expected to change (Goodale *et al.*, 2002; Le Quéré *et al.*, 2009), and this can benefit the estimation of the annual carbon budget.

Literature Cited

Adams WW, Demmig-Adams B, Rosenstiel TN, Brightwell AK, Ebbert V. 2002. Photosynthesis and photoprotection in overwintering plants. *Plant Biology* **4**(5): 545-557.

Adams WW, Zarter CR, Ebbert V, Demmig-Adams B. 2004. Photoprotective strategies of overwintering evergreens. *Bioscience* **54**(1): 41-49.

Apps MJ, Kurz WA, Luxmoore RJ, Nilsson LO, Sedjo RA, Schmidt R, Simpson LG, Vinson TS. 1993. Boreal forests and tundra. *Water Air and Soil Pollution* **70**(1-4): 39-53.

Baker NR. 2008. Chlorophyll fluorescence: A probe of photosynthesis in vivo. *Annual Review of Plant Biology*, 89-113.

Barton CVM, North PRJ. 2001. Remote sensing of canopy light use efficiency using the photochemical reflectance index - Model and sensitivity analysis. *Remote Sensing of Environment* **78**(3): 264-273.

Bigras FJ, Colombo SJ. 2001. *Conifer cold hardiness*. Dordrecht: Kluwer.

Björkman O, Demmig-Adams B. 1994. Regulation of photosynthetic light energy capture, conversion, and dissipation in leaves of higher plants. In: Schulze E-D, Caldwell M eds. *Ecophysiology of Photosynthesis*: Springer Berlin Heidelberg, 17-47.

Butler WL. 1978. Energy distribution in photochemical apparatus of photosynthesis. *Annual Review of Plant Physiology and Plant Molecular Biology* **29**: 345-378.

Canadell JG, Le Quéré C, Raupach MR, Field CB, Buitenhuis ET, Ciais P, Conway TJ, Gillett NP, Houghton RA, Marland G. 2007. Contributions to accelerating atmospheric CO_2 growth from economic activity, carbon intensity, and efficiency of natural sinks. *Proceedings of the National Academy of Sciences of the United States of America* **104**(47): 18866-18870.

Ciais P, Tans PP, Trolier M, White JWC, Francey RJ. 1995. A large northern-hemisphere terrestrial CO_2 sink indicated by the C-13/C-12 ratio of atmospheric CO_2. *Science* **269**(5227): 1098-1102.

Demmig-Adams B, Adams WW. 1996. The role of xanthophyll cycle carotenoids in the protection of photosynthesis. *Trends in Plant Science* **1**(1): 21-26.

Ensminger I, Sveshnikov D, Campbell DA, Funk C, Jansson S, Lloyd J, Shibistova O, Öquist G. 2004. Intermittent low temperatures constrain spring recovery of photosynthesis in boreal Scots pine forests. *Global Change Biology* **10**(6): 995-1008.

Filella I, Porcar-Castell A, Munné-Bosch S, Bäck J, Garbulsky MF, Peñuelas J. 2009. PRI assessment of long-term changes in carotenoids/chlorophyll ratio and short-term changes in de-epoxidation state of the xanthophyll cycle. *International Journal of Remote Sensing* **30**(17): 4443-4455.

Frankenberg C, Fisher JB, Worden J, Badgley G, Saatchi SS, Lee JE, Toon GC, Butz A, Jung M, Kuze A, Yokota T. 2011. New global observations of the terrestrial carbon cycle from GOSAT: Patterns of plant fluorescence with gross primary productivity. *Geophysical Research Letters* **38**.

Gamon JA, Berry JA. 2012. Facultative and constitutive pigment effects on the Photochemical Reflectance Index (PRI) in sun and shade conifer needles. *Israel Journal of Plant Sciences* **60**(1-2): 85-95.

Garrity SR, Eitel JUH, Vierling LA. 2011. Disentangling the relationships between plant pigments and the photochemical reflectance index reveals a new approach for remote estimation of carotenoid content. *Remote Sensing of Environment* **115**(2): 628-635.

Gilmore AM, Ball MC. 2000. Protection and storage of chlorophyll in overwintering evergreens. *Proceedings of the National Academy of Sciences of the United States of America* **97**(20): 11098-11101.

Goodale CL, Apps MJ, Birdsey RA, Field CB, Heath LS, Houghton RA, Jenkins JC, Kohlmaier GH, Kurz W, Liu SR, Nabuurs GJ, Nilsson S, Shvidenko AZ. 2002. Forest carbon sinks in the Northern Hemisphere. *Ecological Applications* **12**(3): 891-899.

Horton P, Ruban AV, Walters RG. 1996. Regulation of light harvesting in green plants. *Annual Review of Plant Physiology and Plant Molecular Biology* **47**: 655-684.

Hüner NPA, Öquist G, Sarhan F. 1998. Energy balance and acclimation to light and cold. *Trends in Plant Science* **3**(6): 224-230.

IPCC. 2007. Solomon S, Qin M, Manning M, Chen Z, Marquis M, Averyt KB, Tignor M, Miller HL, eds. *Climate Change 2007: The Physical Science Basis. Working Group I to the Fourth Assessment Report of the Intergovernmental Panel on Climate Change.* Cambridge, UK: Cambridge University Press.

Kurz WA, Apps MJ. 1999. A 70-year retrospective analysis of carbon fluxes in the Canadian forest sector. *Ecological Applications* **9**(2): 526-547.

Kurz WA, Stinson G, Rampley GJ, Dymond CC, Neilson ET. 2008. Risk of natural disturbances makes future contribution of Canada's forests to the global carbon cycle highly uncerain. *Proceedings of the National Academy of Sciences of the United States of America* **105**(5): 1551-1555.

Le Quéré C, Raupach MR, Canadell JG, Marland G, Bopp L, Ciais P, Conway TJ, Doney SC, Feely RA, Foster P, Friedlingstein P, Gurney K, Houghton RA, House JI, Huntingford C, Levy PE, Lomas MR, Majkut J, Metzl N, Ometto JP, Peters GP, Prentice IC, Randerson JT, Running SW, Sarmiento JL, Schuster U, Sitch S, Takahashi T, Viovy N, van der Werf GR, Woodward FI. 2009. Trends in the sources and sinks of carbon dioxide. *Nature Geoscience* **2**(12): 831-836.

Levitt J. 1980. *Responses of plants to environmental stresses*. New York: Academic Press.

Maxwell K, Johnson GN. 2000. Chlorophyll fluorescence: A practical guide. *Journal of Experimental Botany* **51**(345): 659-668.

Meroni M, Rossini M, Guanter L, Alonso L, Rascher U, Colombo R, Moreno J. 2009. Remote sensing of solar-induced chlorophyll fluorescence:

Review of methods and applications. *Remote Sensing of Environment* **113**(10): 2037-2051.

Nichol CJ, Huemmrich KF, Black TA, Jarvis PG, Walthall CL, Grace J, Hall FG. 2000. Remote sensing of photosynthetic-light-use efficiency of boreal forest. *Agricultural and Forest Meteorology* **101**(2-3): 131-142.

Nichol CJ, Lloyd J, Shibistova O, Arneth A, Roser C, Knohl A, Matsubara S, Grace J. 2002. Remote sensing of photosynthetic-light-use efficiency of a Siberian boreal forest. *Tellus Series B-Chemical and Physical Meteorology* **54**(5): 677-687.

Öquist G, Hüner NPA. 2003. Photosynthesis of overwintering evergreen plants. *Annual Review of Plant Biology* **54**: 329-355.

Ottander C, Campbell D, Öquist G. 1995. Seasonal changes in photosystem II organization and pigment composition in *Pinus sylvestris*. *Planta* **197**(1): 176-183.

Pan YD, Birdsey RA, Fang JY, Houghton R, Kauppi PE, Kurz WA, Phillips OL, Shvidenko A, Lewis SL, Canadell JG, Ciais P, Jackson RB, Pacala SW, McGuire AD, Piao SL, Rautiainen A, Sitch S, Hayes D. 2011. A Large and Persistent Carbon Sink in the World's Forests. *Science* **333**(6045): 988-993.

Porcar-Castell A. 2011. A high-resolution portrait of the annual dynamics of photochemical and non-photochemical quenching in needles of *Pinus sylvestris*. *Physiologia Plantarum* **143**(2): 139-153.

Porcar-Castell A, Garcia-Plazaola JI, Nichol CJ, Kolari P, Olascoaga B, Kuusinen N, Fernandez-Marín B, Pulkkinen M, Juurola E, Nikinmaa E. 2012. Physiology of the seasonal relationship between the photochemical reflectance index and photosynthetic light use efficiency. *Oecologia* **170**(2): 313-323.

Powles SB. 1984. Photoinhibition of photosynthesis induced by visible light. *Annual Review of Plant Physiology and Plant Molecular Biology* **35**: 15-44.

Sims DA, Gamon JA. 2002. Relationships between leaf pigment content and spectral reflectance across a wide range of species, leaf structures and developmental stages. *Remote Sensing of Environment* **81**(2-3): 337-354.

Stylinski CD, Gamon JA, Oechel WC. 2002. Seasonal patterns of reflectance indices, carotenoid pigments and photosynthesis of evergreen chaparral species. *Oecologia* **131**(3): 366-374.

Thayer SS, Björkman O. 1990. Leaf xanthophyll content and composition in sun and shade determined by HPLC. *Photosynthesis Research* **23**(3): 331-343.

Thurner M, Beer C, Santoro M, Carvalhais N, Wutzler T, Schepaschenko D, Shvidenko A, Kompter E, Ahrens B, Levick SR, Schmullius C. 2014. Carbon stock and density of northern boreal and temperate forests. *Global Ecology and Biogeography* **23**(3): 297-310.

Verhoeven A. 2014. Sustained energy dissipation in winter evergreens. *New Phytologist* **201**(1): 57-65.

Verhoeven AS. 2013. Recovery kinetics of photochemical efficiency in winter stressed conifers: the effects of growth light environment, extent of the season and species. *Physiologia Plantarum* **147**(2): 147-158.

Verhoeven AS, Adams WW, Demmig-Adams B. 1996. Close relationship between the state of the xanthophyll cycle pigments and photosystem II efficiency during recovery from winter stress. *Physiologia Plantarum* **96**(4): 567-576.

Verhoeven AS, Adams WW, Demmig-Adams B. 1999. The xanthophyll cycle and acclimation of *Pinus ponderosa* and *Malva neglecta* to winter stress. *Oecologia* **118**(3): 277-287.

Vogg G, Heim R, Hansen J, Schäfer C, Beck E. 1998. Frost hardening and photosynthetic performance of Scots pine (*Pinus sylvestris* L.) needles. I. Seasonal changes in the photosynthetic apparatus and its function. *Planta* **204**(2): 193-200.

Chapter 4. Implications for Remote Sensing

Introduction

Optical sampling (spectral reflectance) provides a technique that can be utilized at various spatial scales to monitor plant physiological activity in response to environmental conditions. Reflectance can be applied to individual leaves, canopies, and ecosystems as a whole. Leaf level measurements provide a direct method to probe the pigment composition. Larger spatial scales introduce more variables that can affect reflectance such as canopy structure, background materials, atmospheric absorption, sun and sensor angle and cloud cover (Barton & North, 2001; Gamon *et al.*, 2007). At larger spatial scales, these confounding factors may affect our interpretation of remotely sensed data, so it is not always clear if physiological interpretations of the PRI at the leaf scale apply at larger scales.

Previous chapters focused on leaf level responses for potted seedlings of two species, leaving open the question of whether these responses are seen in other species or larger scales. Stylinski *et al.* (2002) reported that the PRI detects pigment changes of the xanthophyll cycle and total pool size at the leaf and canopy level. Previous studies have shown that for closed-canopy stands, there are parallel leaf and canopy PRI responses (Gamon & Qiu, 1999; Stylinski *et al.*, 2002). Leaves at the top of the canopy experience similar incoming irradiance and temperature levels, which are the primary factors driving pigment composition. These leaves are the primary targets at canopy scale measurements so might we expect to see parallel changes in the PRI at the leaf and canopy scale, providing other confounding factors are not dominating.

The focus of this chapter was to evaluate the seasonal PRI transitions detected in previous chapters at broader contexts. We examined the spring activation of the PRI at both the leaf and canopy scales to see if the spring PRI transition was also visible at a larger spatial scale. Additional evergreen species were also monitored to assess the seasonal transition in other evergreen conifers.

Materials and Methods

The same Lodgepole pine (*Pinus contorta* D.) and Ponderosa pine (*Pinus ponderosa* Laws.) seedlings were used from previous chapters. Potted white spruce (*Picea glauca* Voss) were planted during the summer of 2011 in small 2.31 L pots (CP412CH, Stuewe & Sons, Tangent, OR, USA) in a 1:2 soil mixture of sandy top soil and sunshine mix (Sunshine Mix 4, Sun Gro Horticulture, Agawam, MA, USA) with added slow release fertilizer (Nutricote 14-14-14, Sun Gro Horticulture, Agawam, MA, USA). The potted plants were arranged in synthetic, closed-canopy stands and kept under the same watering and winter insulation regime. Mature *P. contorta* in the ground at the University of Alberta campus were also monitored.

Leaf scale spectral measurements were performed the same as the previous chapters. *P. contorta* and *P. ponderosa* used an identical sampling regime with a sample size of 30 measurements per sampling date (5 leaves per plant, 6 plants). For *P. glauca*, two random leaves per plant from the top of the canopy were sampled from seven different plants, providing a total sample size of 14. For the mature *P. contorta*, five random leaves exposed to the sun were measured per plant from five different plants, providing a total sample size of 25. The PRI was calculated and averaged together for each sample date.

$$PRI = \frac{R_{531} - R_{570}}{R_{531} + R_{570}} \qquad (1)$$

Stand-scale measurements were collected using a duel channel field spectrometer (Uni-Spec-DC, PP Systems, Amesbury, MA, USA) equipped with two fibre optics. An upwards facing fibre (UNI686, PP Systems, Amesbury, MA, USA) was attached to a cosine receptor (UNI435, PP Systems, Amesbury, MA, USA) for incoming irradiance. A downwards looking fibre (UNI684, PP Systems, Amesbury, MA, USA) was fitted with a field-of-view restrictor (UNI688, PP Systems, Amesbury, MA, USA) to limit the field-of-view to approximately 20 º. Measurements on the potted P. contorta and P. ponderosa were performed approximately 0.5 m above the top of the canopy. The PRI was calculated using Eq. 1. For each species, 12 measurements were taken with the fibre pointed at different sections of the canopy and averaged together.

The spring recovery of the PRI was monitored from 27 March 2013 to 17 July 2013 on an approximately weekly interval. Data collection from 13:00 to 14:00 (within an hour of solar noon) was to ensure the presence of maximum sunlight and reduce diurnal variability. The facultative process at the leaf scale was examined on 4 June 2013 by measuring the absolute diurnal change of the

PRI. Pre-dawn measurements were completed an hour before sunrise and afternoon measurements near solar noon for dark- and light-adapted leaves.

Results

The PRI at the leaf and canopy scales exhibited parallel patterns during spring recovery (Fig. 4-1). Lowest PRI values during the late winter season during late March and early April transitioned over four weeks into high summer values for the remainder of the sampling period. Leaf and canopy scale PRI had significant correlations for all sampling dates in *P. contorta* (r^2 = 0.971, $p<0.0001$) and *P. ponderosa* (r^2 = 0.800, $p<0.001$) (Fig. 4-2).

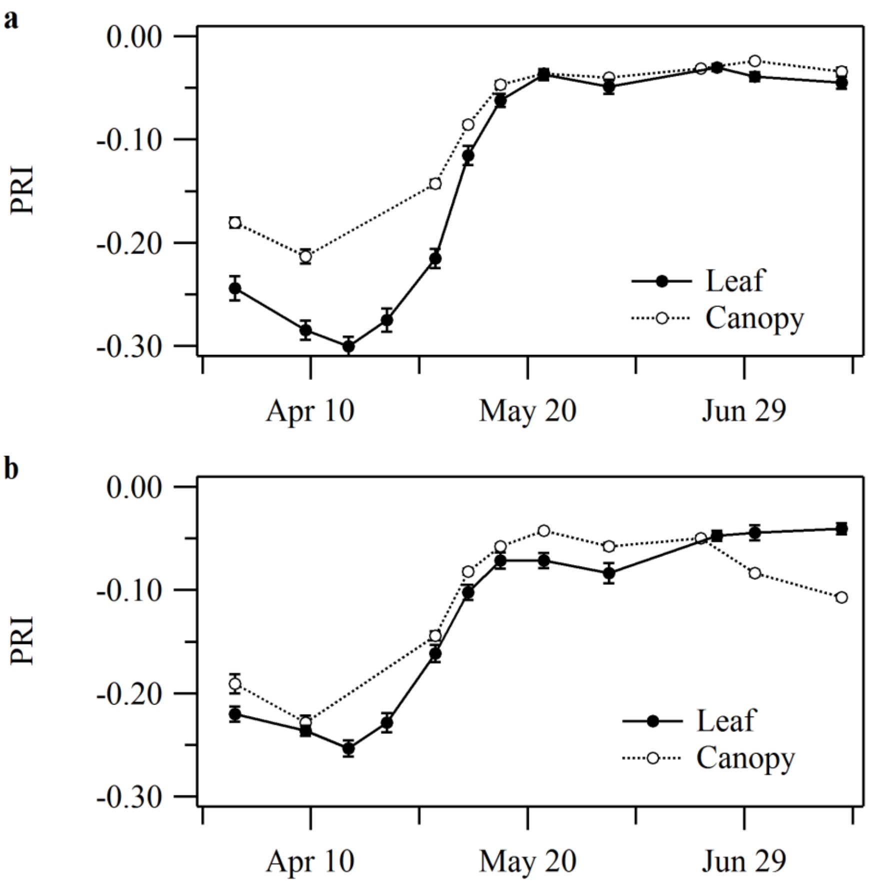

Figure 4-1. The 2013 spring recovery of the PRI at the leaf and canopy scale for *P. contorta* (a) and *P. ponderosa* (b). Error bars denote standard error of the mean.

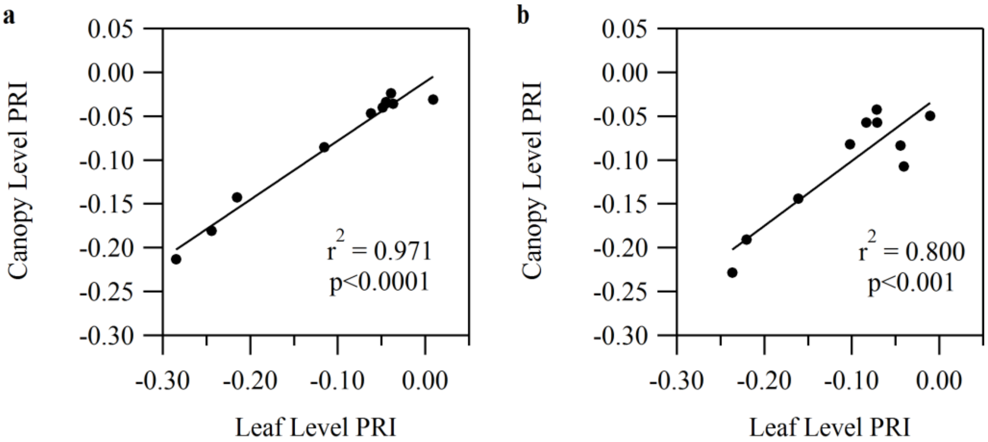

Figure 4-2. The 2013 spring recovery correlations of the PRI between leaf and stand level measurements for *P. contorta* (a) and *P. ponderosa* (b). (n = 10)

Three different evergreen species exhibited parallel spring recovery of the PRI (Fig. 4-3a). Stable winter values are shown during early April. Transition of the PRI occurred over four weeks, followed by summer values that remained stable for the rest of the experiment. The *P. contorta* seedling and adult cohorts also exhibited parallel spring recovery (Fig. 4-3a). Some deviations between the different ages are seen during the winter and transitional periods, but the summer values are very similar. The facultative process is present in all species and age groups (Fig. 4-3b). Dark-adapted leaves have high PRI values, while light-adapted leaves have lower PRI values. The absolute change between dark- and light-adapted PRI values are approximately 0.03, which is much smaller than the constitutive seasonal change at approximately 0.25.

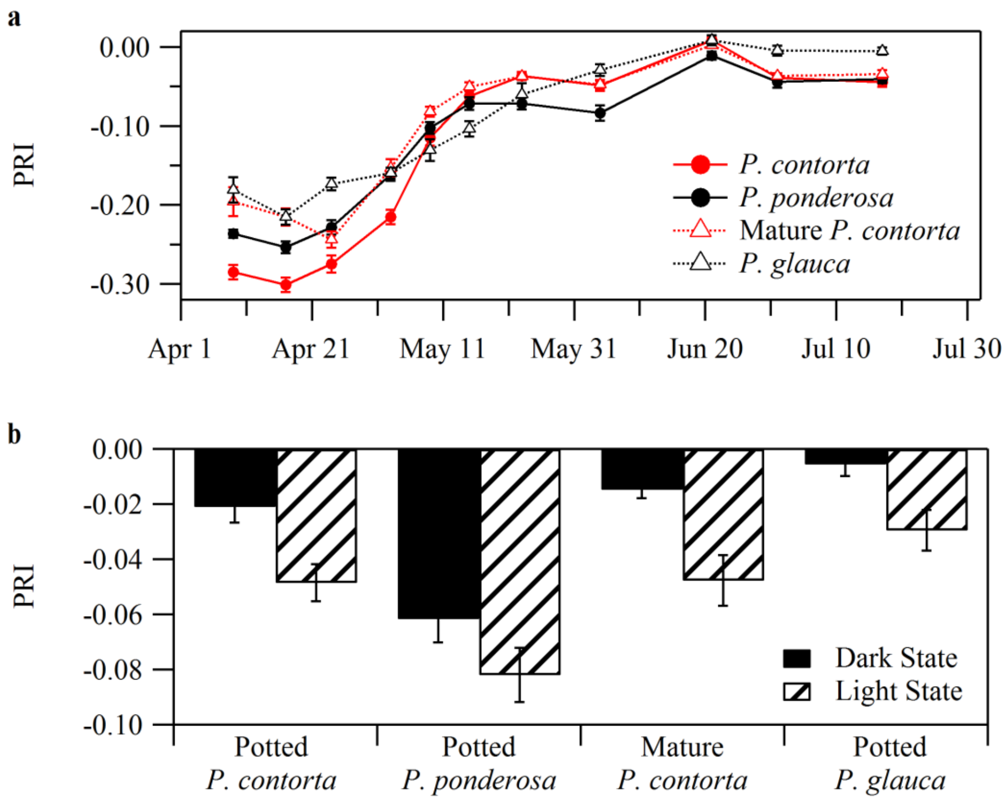

Figure 4-3. Three evergreen species exhibited similar seasonal and diurnal responses at the leaf level. The 2013 spring recovery had large winter to summer transition of the PRI (a). Absolute diurnal response from dark- to light-adapted leaves measured on 2013 June 03 (b). Error bars denote standard error of the mean.

Discussion

Synchrony in the leaf and closed-canopy stand responses shows that the PRI detects similar mechanisms at the two scales, which is similar to other studies (Gamon & Qiu, 1999; Stylinski *et al.*, 2002). The large change between the winter and summer values provide clear signals that can be detected at larger spatial scales. Using the PRI to quantify pigment features for photosynthetic activity is still unclear since the PRI values show variation between spatial scales within the same canopy. These variations are likely caused by any number of confounding factors, which introduces additional implications affecting reflectance measurements (Barton & North, 2001).

A number of evergreen conifers in boreal climate undergo seasonal pigment changes to survive a range of environmental conditions (Öquist & Hüner, 2003; Adams *et al.*, 2004; Verhoeven, 2014). The PRI is able to detect these changes in three different species during this experiment suggesting that other evergreens can be monitored as well. This response was not an artificial process due to their potted setting since mature *P. contorta* in a more natural setting also exhibited similar responses. Regardless of species and age, the PRI acts as a valid indicator of carotenoid:chlorophyll ratios in boreal evergreens that undergo strong seasonality.

These results show the applicability of the leaf level PRI measurements from the previous chapters and demonstrate that it can be scaled up from leaves to the canopy. The ability to detect leaf traits at stands scales has been controversial (Knyazikhin *et al.*, 2013; Townsend *et al.*, 2013), but these results suggest we can indeed detect changing leaf physiology at stand levels. Boreal forests are dominantly made up of evergreen conifers, which can be expected to undergo large seasonal changes that the PRI can detect. Utilizing the PRI at larger scales can provide a physiological signal of the transitions between winter downregulated and summer growth states. Detecting when evergreens turn "on and off" photosynthetically can help determine growing season length, an important factor in annual carbon sequestration.

Literature Cited

Adams WW, Zarter CR, Ebbert V, Demmig-Adams B. 2004. Photoprotective strategies of overwintering evergreens. *Bioscience* **54**(1): 41-49.

Barton CVM, North PRJ. 2001. Remote sensing of canopy light use efficiency using the photochemical reflectance index - Model and sensitivity analysis. *Remote Sensing of Environment* **78**(3): 264-273.

Gamon JA, Qiu H. 1999. Ecological applications of remote sensing at multiple scales. In: Pugnaire FI, Valladares F eds. *Handbook of Functional Plant Ecology*. New York: Marcel Dekker, Inc., 805-846.

Gamon JA, Qiu H, Sanchez-Azofeifa A. 2007. Ecological Applications of Remote Sensing at Multiple Scales. *Functional Plant Ecology, Second Edition*: CRC Press.

Knyazikhin Y, Schull MA, Stenberg P, Möttus M, Rautiainen M, Yang Y, Marshak A, Carmona PL, Kaufmann RK, Lewis P, Disney MI, Vanderbilt V, Davis AB, Baret F, Jacquemoud S, Lyapustin A, Myneni RB. 2013. Hyperspectral remote sensing of foliar nitrogen content. *Proceedings of the National Academy of Sciences of the United States of America* **110**(3): E185-E192.

Öquist G, Hüner NPA. 2003. Photosynthesis of overwintering evergreen plants. *Annual Review of Plant Biology* **54**: 329-355.

Stylinski CD, Gamon JA, Oechel WC. 2002. Seasonal patterns of reflectance indices, carotenoid pigments and photosynthesis of evergreen chaparral species. *Oecologia* **131**(3): 366-374.

Townsend PA, Serbin SP, Kruger EL, Gamon JA. 2013. Disentangling the contribution of biological and physical properties of leaves and canopies in imaging spectroscopy data. *Proceedings of the National Academy of Sciences of the United States of America* **110**(12): E1074-E1074.

Verhoeven A. 2014. Sustained energy dissipation in winter evergreens. *New Phytologist* **201**(1): 57-65.

Chapter 5: General Conclusions

One objective was to clarify the long-term seasonal (constitutive) and short-term diurnal (facultative) responses of the PRI in evergreen species exposed to natural seasonal cycles. We found that, over the study period, the PRI actually exhibited three types of responses to changing temperature and irradiance. The largest response occurred between summer and winter, with highest values in the summer and lowest in the winter. The smallest response involved the short-term diurnal cycle exhibiting highest PRI values at pre-dawn, and lowest near solar noon. A third, previously unreported response occurred during transitions of temperature from cold winter days (0 to -5 °C) to deep cold days (<-5 °C), which may have involved ultra-structural changes affecting leaf optical properties. These findings clarify that the constitutive response of the PRI was driven by carotenoid:chlorophyll ratios (Stylinski *et al.*, 2002; Filella *et al.*, 2009; Garrity *et al.*, 2011) and the facultative response detected changes in the xanthophyll cycle (Peñuelas *et al.*, 1995; Gamon *et al.*, 1997). The constitutive and facultative responses were detected by the PRI in all three different evergreen species tested, suggesting that this may be a general response of evergreens. Prior to this study, our knowledge of the sources of variation in the PRI relied heavily on assumptions that the PRI was driven by a single physiological response (constitutive or facultative), which does not consider a potential overlap. The results of this study suggest that future studies of the PRI response over seasonal cycles should consider both these PRI responses.

The PRI was found to track photosynthetic activity during spring recovery, a key period when evergreens reactivate photosynthetically for growth. It had significant correlations with other photosynthetic metrics from chlorophyll fluorescence and gas exchange. Variations were caused from differences in kinetics because of the mechanistic differences driving each metric. The facultative xanthophyll cycle component, recovered soonest. Photosystem II was next to recover, and the constitutive carotenoid:chlorophyll ratio component was last to recover. Gas exchange recovered the most gradually and fully recovered after all the other components. Photosynthesis and photoprotection rely on a number of different mechanisms ensuring suitable energy balance under stressful conditions (Demmig-Adams & Adams, 1992; Björkman & Demmig-Adams, 1994; Öquist & Hüner, 2003). This study did not look at the role of photosystem I (Sonoike, 2011) and the lutein cycle (García-Plazaola *et al.*, 2003; Matsubara *et al.*, 2005; García-Plazaola *et al.*, 2007; Jahns & Holzwarth, 2012) in energy dissipation. Differences in kinetics between mechanisms are likely due to time and energy constraints for seasonal transition; xanthophyll cycle activity can recover quickly, but pigment pools are more expensive and take time and energy to build. Different kinetics could also act as a safeguard to unexpected declines in temperature during spring recovery that could potentially harm the transitional leaves.

This study demonstrated that the PRI could monitor the seasonal activation and deactivation of photosynthesis. Measuring the transition of photosynthesis can be utilized to determine growing season length, which affects annual carbon sequestration. Season length is expected to change (Xu *et al.*, 2013), and the outcome of these changes on annual carbon dynamics are not well understood (Ensminger *et al.*, 2004; Euskirchen *et al.*, 2006; Richardson *et al.*, 2010). A longer growing season is generally expected to increase carbon sequestration, but can also lead to reduced sequestration if summer stresses occur (Kurz *et al.*, 2008). Variations in spring recovery may have carry-over effects into the autumn downregulation season (Richardson *et al.*, 2010), which adds further implications and uncertainties to how changing spring and autumn transitions may affect annual productivity. Utilizing the PRI (or a similar index) to detect the activation and deactivation of photosynthetic activity could help explore climate change on productivity. Future studies could attempt to fully quantify the PRI as a measure of photosynthetic rate or LUE, but must be consider potential variations between species.

The PRI is an optically derived index that can be detected with remote sensing at larger spatial scales. Studies at the ecosystem scale have shown the capability of the PRI to detect photosynthetic activity (Rahman *et al.*, 2001; Garbulsky *et al.*, 2011; Peñuelas *et al.*, 2011; Garbulsky *et al.*, 2013). However, lack of ground validation can result in the misinterpretation of the physiological mechanisms driving the PRI and the misunderstanding of its association with LUE and photosynthetic activity. Remote sensing at larger scales introduce more variations to the PRI (Barton & North, 2001), so understanding the physiological mechanisms affecting the constitutive and facultative component can help clarify some of the causes of variation in the PRI. In our study, linking leaf level to canopy level measurements demonstrated that the constitutive PRI response is consistent across species and different scales. Consideration of the temporal context between constitutive and facultative processes can improve our interpretation of the PRI and its association to photosynthetic activity. The differences in spectral responses at different temporal scales could be examined to develop an alternate index (or combination of index formulations) to differentiate the different responses.

The boreal forests are undergoing climate change with shifting temperatures, altered timing of seasonal transitions, and increased frequency of disturbances (Goodale *et al.*, 2002; Kurz *et al.*, 2008; IPCC, 2013). These changes lead to uncertainty of the boreal forests' source/sink dynamics, and optical monitoring (from the ground and from satellites) could help address this question. Satellites such as the Aqua and Terra Moderate Resolution Imaging Spectroradiometer (MODIS) have built up almost 15 years of data that can calculate a PRI or similar index. This could provide large scale historical trends and be utilized for frequent measurements to improve current models and assist in monitoring carbon balance.

Literature Cited

Barton CVM, North PRJ. 2001. Remote sensing of canopy light use efficiency using the photochemical reflectance index - Model and sensitivity analysis. *Remote Sensing of Environment* **78**(3): 264-273.

Björkman O, Demmig-Adams B 1994. Regulation of photosynthetic light energy capture, conversion, and dissipation in leaves of higher plants. In: Schulze E-D, Caldwell M eds. *Ecophysiology of Photosynthesis*: Springer Berlin Heidelberg, 17-47.

Demmig-Adams B, Adams WW. 1992. Photoprotection and other responses of plants to high light stress. *Annual Review of Plant Physiology and Plant Molecular Biology* **43**: 599-626.

Ensminger I, Sveshnikov D, Campbell DA, Funk C, Jansson S, Lloyd J, Shibistova O, Öquist G. 2004. Intermittent low temperatures constrain spring recovery of photosynthesis in boreal Scots pine forests. *Global Change Biology* **10**(6): 995-1008.

Euskirchen ES, McGuire AD, Kicklighter DW, Zhuang Q, Clein JS, Dargaville RJ, Dye DG, Kimball JS, McDonald KC, Melillo JM, Romanovsky VE, Smith NV. 2006. Importance of recent shifts in soil thermal dynamics on growing season length, productivity, and carbon sequestration in terrestrial high-latitude ecosystems. *Global Change Biology* **12**(4): 731-750.

Filella I, Porcar-Castell A, Munné-Bosch S, Bäck J, Garbulsky MF, Peñuelas J. 2009. PRI assessment of long-term changes in carotenoids/chlorophyll ratio and short-term changes in de-epoxidation state of the xanthophyll cycle. *International Journal of Remote Sensing* **30**(17): 4443-4455.

Gamon JA, Serrano L, Surfus JS. 1997. The photochemical reflectance index: an optical indicator of photosynthetic radiation use efficiency across species, functional types, and nutrient levels. *Oecologia* **112**(4): 492-501.

Garbulsky MF, Peñuelas J, Gamon JA, Inoue Y, Filella I. 2011. The photochemical reflectance index (PRI) and the remote sensing of leaf, canopy and ecosystem radiation use efficiencies A review and meta-analysis. *Remote Sensing of Environment* **115**(2): 281-297.

Garbulsky MF, Peñuelas J, Ogaya R, Filella I. 2013. Leaf and stand-level carbon uptake of a Mediterranean forest estimated using the satellite-derived reflectance indices EVI and PRI. *International Journal of Remote Sensing* **34**(4): 1282-1296.

García-Plazaola JI, Hernàndez A, Olano JM, Becerril JM. 2003. The operation of the lutein epoxide cycle correlates with energy dissipation. *Functional Plant Biology* **30**(3): 319-324.

García-Plazaola JI, Matsubara S, Osmond CB. 2007. Review: The lutein epoxide cycle in higher plants: its relationships to other xanthophyll cycles and possible functions. *Functional Plant Biology* **34**(9): 759-773.

Garrity SR, Eitel JUH, Vierling LA. 2011. Disentangling the relationships between plant pigments and the photochemical reflectance index reveals a new approach for remote estimation of carotenoid content. *Remote Sensing of Environment* **115**(2): 628-635.

Goodale CL, Apps MJ, Birdsey RA, Field CB, Heath LS, Houghton RA, Jenkins JC, Kohlmaier GH, Kurz W, Liu SR, Nabuurs GJ, Nilsson S, Shvidenko AZ. 2002. Forest carbon sinks in the Northern Hemisphere. *Ecological Applications* **12**(3): 891-899.

IPCC 2013. Climate Change 2013: The Physical Science Basis. Contribution of Working Group I to the Fifth Assessment Report of the Intergovernmental Panel on Climate Change.In Stocker TF, Qin D, Plattner GK, Tignor M, Allen SK, Boschung T, Nauels A, Xia Y, Bex V, Midgley PM. Cambridge, UK.

Jahns P, Holzwarth AR. 2012. The role of the xanthophyll cycle and of lutein in photoprotection of photosystem II. *Biochimica Et Biophysica Acta-Bioenergetics* **1817**(1): 182-193.

Kurz WA, Stinson G, Rampley GJ, Dymond CC, Neilson ET. 2008. Risk of natural disturbances makes future contribution of Canada's forests to the global carbon cycle highly uncerain. *Proceedings of the National Academy of Sciences of the United States of America* **105**(5): 1551-1555.

Matsubara S, Naumann M, Martin R, Nichol C, Rascher U, Morosinotto T, Bassi R, Osmond B. 2005. Slowly reversible de-epoxidation of lutein-epoxide in deep shade leaves of a tropical tree legume may 'lock-in' lutein-based photoprotection during acclimation to strong light. *Journal of Experimental Botany* **56**(411): 461-468.

Öquist G, Hüner NPA. 2003. Photosynthesis of overwintering evergreen plants. *Annual Review of Plant Biology* **54**: 329-355.

Peñuelas J, Filella I, Gamon JA. 1995. Assessment of photosynthetic radiation-use efficiency with spectral reflectance. *New Phytologist* **131**(3): 291-296.

Peñuelas J, Garbulsky MF, Filella I. 2011. Photochemical reflectance index (PRI) and remote sensing of plant CO2 uptake. *New Phytologist* **191**(3): 596-599.

Rahman AF, Gamon JA, Fuentes DA, Roberts DA, Prentiss D. 2001. Modeling spatially distributed ecosystem flux of boreal forest using hyperspectral indices from AVIRIS imagery. *Journal of Geophysical Research-Atmospheres* **106**(D24): 33579-33591.

Richardson AD, Black TA, Ciais P, Delbart N, Friedl MA, Gobron N, Hollinger DY, Kutsch WL, Longdoz B, Luyssaert S, Migliavacca M, Montagnani L, Munger JW, Moors E, Piao SL, Rebmann C, Reichstein M, Saigusa N, Tomelleri E, Vargas R, Varlagin A. 2010. Influence of spring and autumn phenological transitions on forest ecosystem productivity. *Philosophical Transactions of the Royal Society B-Biological Sciences* **365**(1555): 3227-3246.

Sonoike K. 2011. Photoinhibition of photosystem I. *Physiologia Plantarum* **142**(1): 56-64.

Stylinski CD, Gamon JA, Oechel WC. 2002. Seasonal patterns of reflectance indices, carotenoid pigments and photosynthesis of evergreen chaparral species. *Oecologia* **131**(3): 366-374.

Xu L, Myneni RB, Chapin FS, Callaghan TV, Pinzon JE, Tucker CJ, Zhu Z, Bi J, Ciais P, Tømmervik H, Euskirchen ES, Forbes BC, Piao SL, Anderson BT, Ganguly S, Nemani RR, Goetz SJ, Beck PSA, Bunn AG, Cao C, Stroeve JC. 2013. Temperature and vegetation seasonality diminishment over northern lands. *Nature Climate Change* **3**(6): 581-586.

Appendix A: Deep Cold Response

Introduction

During the winter season, temperatures below -5 °C caused an abrupt decrease in reflectance that resulted an increase of the PRI. When temperatures increased above -5 °C, reflectance and the PRI returned to normal winter values (see Chapter 2). This deep cold response, to our knowledge, has not been reported and may indicate another means of extreme cold temperature survival for evergreen conifer species. As a test of the deep cold response, supplementary experiments were performed to determine whether it was indeed biological and not instrument malfunction.

Materials and Methods

The leaf level spectrometer from previous chapters was used in these experiments. Leaf albedo was calculated as the sum of reflectance from 400 to 1000 nm. The PRI was calculated as $(R_{531}-R_{570})/(R_{531}+R_{570})$.

Temperature Controlled Growth Chamber

To simulate the deep cold response of a *P. contorta* leaf, a growth chamber was used to artificially control leaf temperatures. The spectrometer was placed outside the chamber, and remained at room temperature, while the fibre optic traversed the chamber through a small port in the wall. During a cold winter day (0 °C), a leaf was placed inside the growth chamber set a 0 °C and allowed to acclimate for 1 hour. Temperatures started decreased -5 ºC every 30 minutes reaching a low of -15 ºC, which was held for one hour. Temperature patterns were then reversed to increase 5 ºC every 30 minutes until returning to 0 ºC. A thermocouple was attached to the leaf and measured leaf temperature every minute. Optical measurements were measured every 30 seconds.

Factorial Temperature Experiment

To evaluate the role of leaf and instrument temperature on the deep cold response, temperature was naturally manipulated. On a -4 °C day, 12 *P. contorta* leaves were measured with the spectrometer located indoors at room temperature with the fibre optic traversed outside to reach the leaves. After the measurements, the leaves were brought indoors to acclimate to room temperatures for 30 minutes, for measurements with both instrument and leaves at warm temperatures. Then the instrument was brought outdoors for cold acclimation for 30 minutes before measuring the warm leaves. Measurements of already cold leaves with the cold instrument were completed last.

Results and Discussion

Simulated temperatures of a leaf using a growth chamber with the instrument located externally at room temperature exhibited reversible albedo and PRI when temperatures crossed a threshold of approximately -4 °C (Fig. A-1). The deep cold response exhibited an immediate step change. Albedo changed by a value of 30 and the PRI change by about 0.4. Rapid temperature change was not ideal for the plant as gradual changes are more likely to occur naturally, which may cause the values to slightly differ from natural observations of the deep cold response.

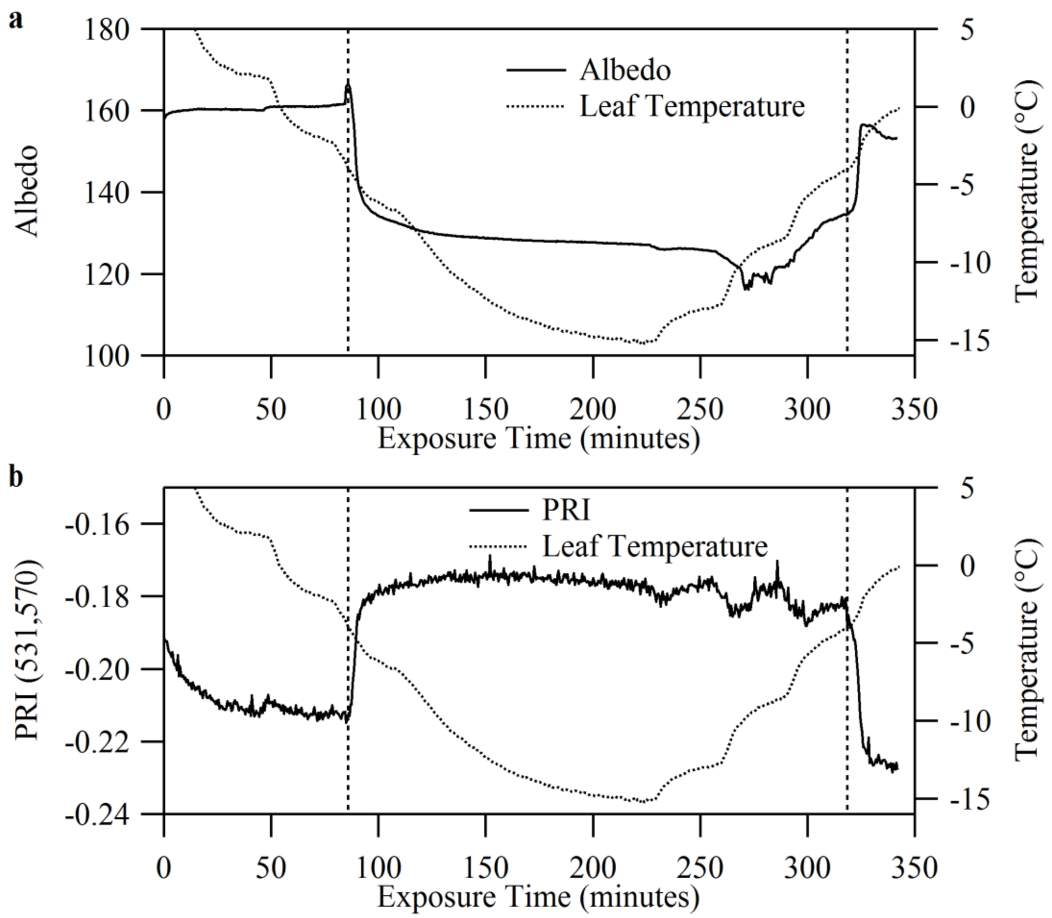

Figure A-1. Artificially imposed temperature treatments (cooling followed by warming) using a growth chamber to simulate the deep cold response in a *P. contorta* needle, while keeping the spectrometer at room temperature. Leaf albedo (a) and the PRI (b) was measured every 30 seconds. A thermocouple was attached to the needle for leaf temperature measured every minute. Vertical dashed line denotes start of transition at -4.0 ºC during cooling and -3.9 ºC during warming.

Alternating outdoor cold (-4 ºC) and warm (room temperature) treatment conditions of leaves and the spectrometer caused abrupt shifts in leaf albedo (Fig. A-2). We observed significant differences across the different leaf temperature treatments for both *P. contorta* (F = 7.164, p<.01) and *P. ponderosa* (F=20.128, p<.0001). In all cases, cold leaves had lower albedo, independent of the instrument temperature. This indicates that leaf temperature is likely to cause the deep cold response and not instrument temperatures.

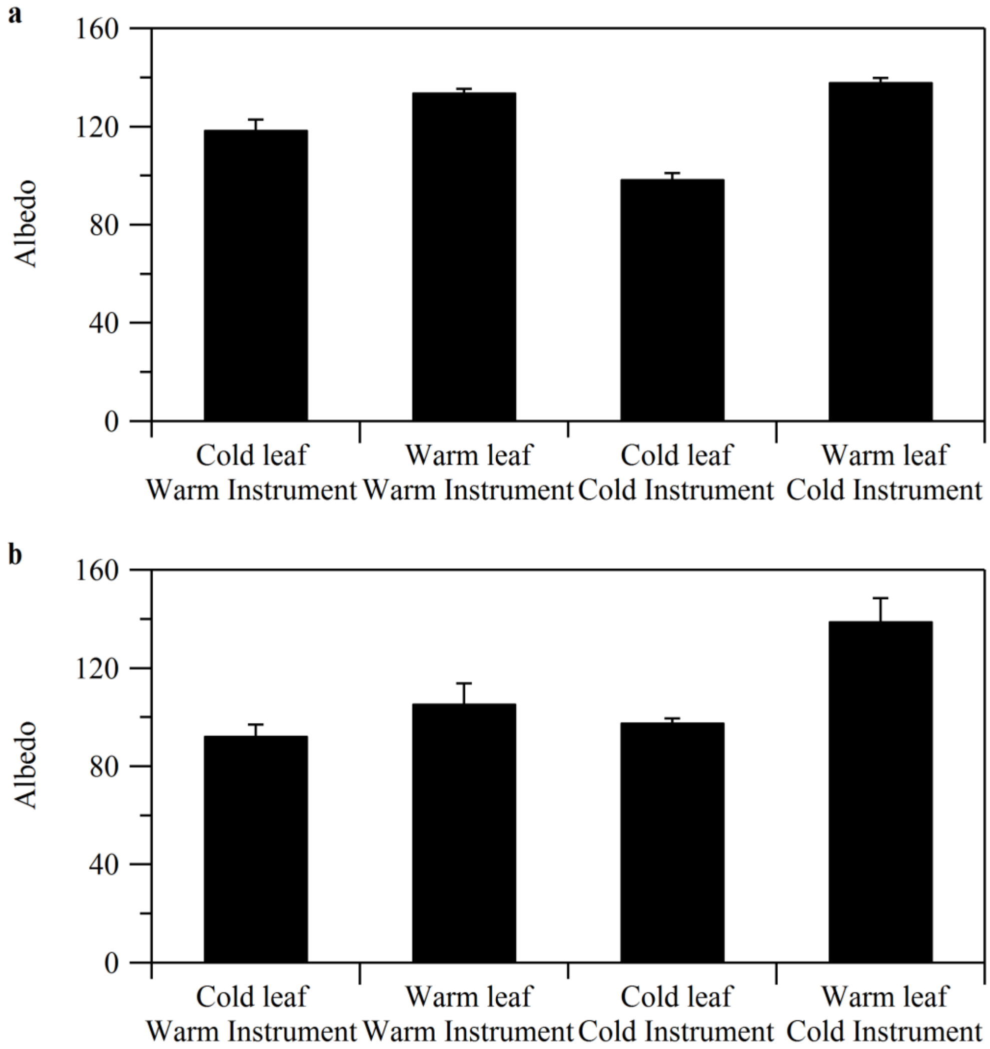

Figure A-2. Experimental tests of the deep cold response of albedo (sum of reflectance from 400 to 1000 nm) for *P. contorta* (a) and *P. ponderosa* (b) under different leaf and instrument temperatures. Sample size is N=12 for each treatment, which were averaged together. Error bars denote standard deviation.

Conclusions

Both experiments exhibited the same pattern of decreased albedo when leaves were at deep cold temperatures. From this we conclude that the deep cold response of evergreen needles is indeed biological. We speculate that decreased albedo is caused from an ultra-structural change (possibly involving freezing and desiccation) that affects leaf optical properties.